FT

UNCLASSIFIED

NRL Report 6091

Electron-Bombardment Damage in Silicon Solar Cells

R. L. STATLER

Electromagnetic Materials Branch
Solid State Division

October 7, 1964

U.S. NAVAL RESEARCH LABORATORY
Washington, D.C.

UNCLASSIFIED

CONTENTS

Abstract	ii
Problem Status	ii
Authorization	ii
INTRODUCTION	1
THEORY	2
Principle of the Solar Cell	2
Electron Damage in Silicon	4
EXPERIMENTAL PROCEDURE	5
Solar-Cell Specimens	5
Irradiation and Dosimetry	6
Measurement Techniques	9
RESULTS	12
Current-Voltage Characteristics	12
Diffusion Length	14
Photovoltaic Spectral Response	16
CONCLUSIONS	16
ACKNOWLEDGMENTS	18
REFERENCES	19

Copies available from Office of Technical Services
Department of Commerce – $1.50

ABSTRACT

A study has been made of the radiation damage in 11 types of silicon solar cells as a result of 1-Mev electron bombardment. Included in the study are p/n cells, n/p cells of different bulk resistivities, planar cells, and drift-field cells. A comparative analysis was made of the radiation-induced degradation in these cells as a function of short-circuit current, maximum power output, minority-carrier diffusion length, and photovoltaic spectral response. The p/n cells were found to be much more sensitive to radiation damage than any type of n/p cells in this investigation. In the n/p cells, there is a definite indication of increasing radiation resistance accompanying increasing values of bulk resistivity, up to 10 ohm-cm. The drift-field solar cells exhibit a further improvement in radiation resistance beyond that of the other types of n/p cells.

PROBLEM STATUS

This is a final report on one phase of the problem; work is continuing on the problem.

AUTHORIZATION

NRL Problem E02-04
BuShips Projects SF-013-12-04-4533 and
SR-007-11-01-0549
NASA Projects S-13991-G and S-4757-G

Manuscript submitted March 5, 1964.

UNCLASSIFIED

ELECTRON-BOMBARDMENT DAMAGE IN SILICON SOLAR CELLS

INTRODUCTION

Silicon photovoltaic cells, commonly called "solar cells," have been used for purposes of electric power production on space vehicles since the launching of the Vanguard I earth satellite in 1958. In such applications, the location of solar cells on the exterior surface of a satellite ordinarily brings about an exposure to charged-particle radiation. Such space radiation encompasses a broad spectrum of energies and a wide range of fluxes resulting from several natural phenomena, the most prominent of which is the Van Allen radiation contained in the geomagnetic field (1). Since the discovery of this radiation environment in 1958, considerable effort has been concentrated on obtaining more detailed knowledge of the existing fluxes and energies. This work has been accompanied by a parallel effort to investigate the effects of radiation on semiconductor materials and devices. The general macroscopic consequence of radiation exposure on solar cells is exhibited as a gradual decrease in power output which eventuates in the electronic malfunctioning of space vehicles and the ultimate cessation of data transmission.

As a result of the high-altitude nuclear explosion on July 9, 1962, by the U.S. Atomic Energy Commission, a large number of fission electrons were injected into and trapped within the geomagnetic field, thereby greatly intensifying the existing electron flux (2). It was found that a direct effect of this increase in the earth's radiation environment was to shorten the lifetimes of several satellites, namely, TRAAC, ARIEL, and TRANSIT IV-B (3), from years to a matter of days. The amount of decrease depended on the solar-cell semiconductor material, the transparent substance shielding the cell, and the margin of overdesign protection incorporated into the power-supply system.

These developments have emphasized the necessity for determining with greater precision the radiation damage to types of solar cells in current use or in a state of development for operation in radiation environments. Furthermore, there is a great need to ascertain which parameters involved in the physical composition and design of cells play a critical role insofar as radiation resistance is concerned.

Evidence has been put forth that n/p cells are more resistant to radiation damage than p/n cells (4). In addition, p-type silicon of higher resistivity has been observed to be less damaged than low-resistivity (about 1 ohm-cm) material for the same incident flux (5). In keeping with these results, and mindful of the significant concentration of electrons in the Mev range in the Van Allen region, a research program was undertaken with the following objectives:

1. To study comparative radiation damage on n/p solar cells commercially available from sources capable of supplying quantity lots from regular production runs

2. To include in the comparative investigation a representative type of commercial p/n cell

3. To examine the relationship between solar-cell base resistivity and radiation-damage rate in a quantitative manner

4. To employ a sufficient number of each type of cell so as to ensure statistically meaningful data

5. To widen the investigation to include several experimental types of solar cells which have a theoretical basis for exhibiting improved radiation resistance characteristics; e.g., solar cells of the drift-field and planar type

6. To minimize the number of experimental variables in the radiation exposure by making certain that all cell samples receive uniform and equal exposure doses and are always in a similar nonradiative environment

7. To ensure accuracy and reproducibility in all measurements through the frequent use of calibrating standards and by means of crosschecking measurements before and after final irradiations with independent photovoltaic observations by the Space Power Technology Branch at Goddard Space Flight Center.

An electron-bombardment energy of 1 Mev was chosen for two principal reasons. First, by far the greatest amount of existent data has been accumulated at this energy; second, the maximum of the electron-energy spectrum in the Van Allen region is near 1 Mev (6).

THEORY

Principle of the Solar Cell

Although no effort will be made to give a detailed discussion of p-n junction theory, a brief description of the photovoltaic effect which governs the operation of solar cells is relevant to an understanding of the effects of radiation damage on these devices. A typical n/p solar cell is a thin slice of p-type silicon crystal which has been grown with a carefully controlled additive impurity, usually boron. The p-n junction is formed approximately 0.5 micron below the surface by the diffusion of an n-type impurity, such as phosphorus or arsenic. A cross-sectional representation of an n/p solar cell is shown in Fig. 1. The p/n cell is prepared in a similar fashion from n-type silicon, with arsenic serving as the additive impurity, and the p-n junction being formed by a diffusion of boron into the surface layer.

When photons of energy greater than 1.1 ev are incident on the cell, each photon absorption results in the liberation of an electron from a valence site in the silicon lattice and the creation of a corresponding hole, both of which are then free to diffuse throughout the crystal. After a period of time, designated as the minority-carrier lifetime, the respective charge carriers will recombine, having traversed a distance called the minority-carrier diffusion length. This length L is related to the lifetime τ by the well-known expression

$$L^2 = D\,\tau \tag{1}$$

where D is the diffusion constant, which has a value of 38 cm^2/sec for electrons in silicon and 13 cm^2/sec for holes (at 300°K). If the minority carriers diffuse into the junction-field region before recombination occurs, they will be swept across the junction and will give rise to a potential whose magnitude depends on the temperature, the built-in field, the number of minority carriers generated, and the leakage across the junction. The voltage resulting from the diffusion of minority carriers across the junction is that which is available at the solar-cell terminals. Electric power may then be extracted from the cell by permitting the junction current to flow into an external circuit through a plated metallic contact on the back surface of the cell and a plated grid on the front surface.

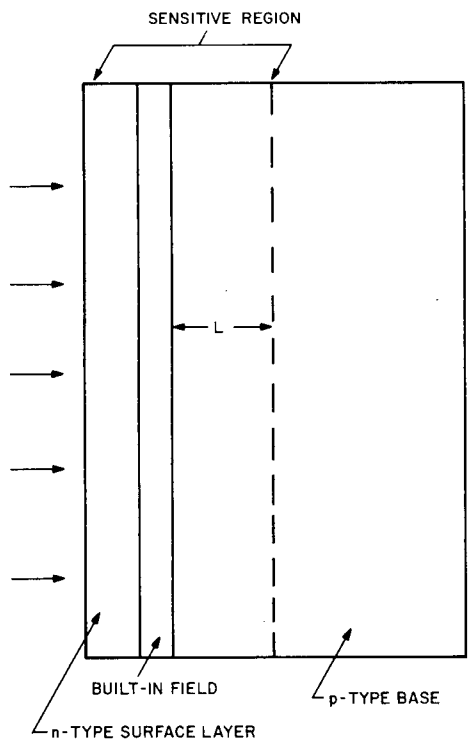

Fig. 1 - Schematic representation of an n/p solar cell

It should be noted that only photons having energies in the range between 1.1 and 3.1 ev are effective in the generation of the junction current in silicon solar cells. Photons of lower energy are not absorbed by means of the photovoltaic process, since the energy required to produce an electron-hole pair is 1.1 ev. These photons contribute solely to the generation of heat within the cell through lattice absorption. On the other hand, the photons with energies in excess of 3.1 ev are either reflected or absorbed within the skin depth of the silicon, as is evident from the published data of absorption coefficients for silicon (7). The minority-carrier surface lifetime, and hence the diffusion length, is several orders of magnitude smaller than the bulk lifetime of the solar cell. Consequently, these minority carriers recombine before reaching the junction.

The current which the solar cell can deliver to a load is given by the expression (8a)

$$I = I_L - I_o \left[\exp (qV/AkT) - 1\right] \qquad (2)$$

where

I = output current

I_L = photon-generated current

I_o = saturation current of the p-n junction

V = generated voltage

q = electronic charge

k = Boltzmann's constant

T = temperature (°K)

A = empirical constant, having a value between 1 and 3.

Under short-circuited load conditions, i.e., $V = 0$, the output current I_{sc} is just equal to the photon-generated current, thereby becoming a measure of overall photon conversion efficiency of the cell. Thus, internal or surface damage which affects the carrier collection efficiency will be manifested by a change in the short-circuit current. Theoretical considerations (9) have shown that the short-circuit current varies as the logarithm of the diffusion length over a range of 10 to 200 microns. Experimental confirmation of this dependence for solar cells of various diffusion lengths has been established (10) by measuring the short-circuit current generated by unfiltered tungsten light.

The open-circuit voltage V_{oc} may be obtained from Eq. (2) by letting $I = 0$, resulting in

$$V_{oc} = (AkT/q) \ln (1 + I_L/I_o) \ . \qquad (3)$$

For the case of large light intensities, i.e., $I_L >> I_o$, this expression becomes

$$V_{oc} = (AkT/q) \ln (I_L/I_o) . \tag{4}$$

The direct dependence of the short-circuit current on the intensity of illumination is indicated in Eq. (2), while Eq. (4) exhibits the logarithmic dependence of the open-circuit voltage on the intensity. Furthermore, the latter relation also shows that V_{oc} is also a function of the saturation current I_o. In view of the fact that the dependence of I_o on the resistivity of the base material has been indicated by a theoretical treatment (8b, 11), it may be shown that the open-circuit voltage will decrease with increasing base resistivity, provided that the other factors remain constant. This has been verified by the empirical relationship reported by Smith, et al. (12).

The maximum power P_{max} which can be delivered by the solar cell is represented as that point on the current-voltage (I-V) characteristic curve for which

$$P_{max} = (I\,V)_{max} = I_m\,V_m \tag{5}$$

where I_m and V_m refer to the current and voltage values for which the product is a maximum. This parameter P_{max} has more significance than does the short-circuit current, from the viewpoint of the application of the solar cell for power conversion. Although P_{max} and I_{sc} are both subject to variations in the surface reflectivity of the solar cell, P_{max} is also a function of the junction characteristics and series resistance of the cell.

Electron Damage in Silicon

The absorption of high-energy electrons by a semiconductor results in the loss of energy by two processes, namely, through production of charge carriers and by the displacement of atoms from normal lattice sites. In the case of 1-Mev electrons incident on a 15-mil-thick silicon solar cell, an average energy of approximately 100 kev per electron is lost through the generation of electron-hole pairs. This estimate is based on the fact that an energy of 3.6 ev is required to generate a single pair (13) and that the generation rate is about 225 pairs per micron (14). In its transit through the cell, an electron may displace a silicon atom from the lattice through the Coulombic interaction with the silicon nuclear charge. The minimum energy required for such a process is 12.9 ev (15), although the average energy imparted to the silicon atom in the collision with 1-Mev electrons is calculated to be 35 ev (16). If the latter energy is available, the silicon atom may be moved a distance several times as great as a lattice spacing, but secondary displacements will not usually be induced by the process. The vacancy thus formed can diffuse through the lattice at room temperatures and is available to combine with impurity atoms to form defect centers. Such centers are thermally stable, and under certain conditions they may serve as minority-carrier recombination sites. The most probable recombination process may be characterized by two separate steps: (a) the trapping of a minority carrier at the defect center, and (b) the subsequent capture of a majority carrier, resulting in the annihilation of the electron-hole pair. Thus, the generation of an increased concentration of new recombination centers leads to a corresponding reduction in the lifetime of minority carriers in silicon.

Although material parameters other than the minority-carrier lifetime are affected by radiation, such as the conductivity and mobility, the effect of 1-Mev electrons on the performance characteristics of solar cells can be related in the main to the decrease in lifetime in the bulk material. The lifetime is governed by the following equation (17):

$$1/\tau = 1/\tau_o + K'\Phi \tag{6}$$

UNCLASSIFIED

where

τ_o = preirradiation minority-carrier lifetime

τ = postirradiation minority-carrier lifetime

Φ = integrated radiation flux

K' = damage constant (a function of the material, the resistivity, the temperature, and the type and energy of the bombarding particle).

If Eq. (1) is utilized, it is seen that the diffusion length will decrease according to

$$1/L^2 = 1/L_o^2 + K\Phi \tag{7}$$

where

$$K = K'/D$$

L_o = preirradiation diffusion length.

For the case of an irradiation which is so prolonged that the condition that $L \ll L_o$ is satisfied,

$$K \approx 1/(L^2\,\Phi) \ . \tag{8}$$

Accordingly, the value of K can be obtained from a one-point measurement, or it may be more accurately determined by plotting $1/L^2$ vs Φ. In this instance, the slope of the resulting straight line is

$$K \equiv d\,(1/L^2)/d\Phi \ . \tag{9}$$

The K value provides a convenient measure for gaging relative radiation damage among various types of solar cells. Furthermore, it affords a useful index for assessing the wide range of damage rates produced in a given type of cell by diverse radiation fields.

EXPERIMENTAL PROCEDURE

Solar-Cell Specimens

The solar cells used in the present study were procured by the Spacecraft Technology Branch of the Goddard Space Flight Center, NASA. In October 1962, all known solar-cell manufacturers were requested to supply lots of 100 n/p silicon cells from their regular production. Each cell was required to have an efficiency of at least 10 percent as measured under a water-filtered 2800°K tungsten light source. Six companies fulfilled the request and furnished cells made from p-type silicon having a resistivity in the range from 1 to 10 ohm-cm. Furthermore, one lot of 100 p/n solar cells with a nominal base resistivity of 1 ohm-cm was obtained from a major supplier. These were chosen for the large amount of existing data on an established type of cell which was representative of the current state of development in this field. Each of the above cells was examined with regard to its current-voltage (I-V) characteristics. The 15 cells in each group of 100 which had I-V values closest to the median of each respective lot were chosen for the investigation.

In addition to these commercial cells, four types of experimental solar cells were also included in the study. The first group comprised 15 n/p planar solar cells, so designated because the techniques conventionally employed in the manufacture of planar semiconductor devices were adapted to their fabrication. Accordingly, the p-n junction is diffused into the surface through a silicon oxide layer which serves a dual purpose. It prevents the edge of the p-n junction from being a region of high dislocation density and also forestalls the possibility of surface contamination. Both conditions are quite possible in the manufacture of conventional solar cells, when the exposed junction edges are etched after the diffusion process is completed.

Next, there were two groups of drift-field cells, furnished by another supplier in accord with the NASA photovoltaic specifications and differing only with respect to the active cell area. Drift-field cells are made by first diffusing a donor-type impurity from the rear surface such that a variation of impurity concentration is achieved in the direction normal to the face. A junction is then diffused in the normal manner from the front surface. The first diffusion process sets up an internal electric field which is proportional to the gradient of the impurity concentration, so that minority carriers are accelerated toward the junction. The net effect of the drift-field process is to increase the probability for carriers to reach the junction before recombination capture. These cells have also been called "graded-base" cells.

Finally, this same manufacturer supplied a group of ten cells made from p-type silicon having a resistivity of 25 ohm-cm and prepared by the same junction diffusion technique as the drift-field cells.

A detailed list of the specimen cells grouped according to type and number is shown in Table 1. A photograph of the cells is shown in Fig. 2.

Table 1
Solar-Cell Specimens Used in the Experiment

Group	Resistivity (ohm-cm)	Type*	Active Area † (cm^2)	Number of Cells
A	1	p/n, com.	1.78	15
B	1	n/p, planar, exp.	3.60	15
C	1	n/p, com.	1.80	15
D	1	n/p, com.	1.70	15
E	25	n/p, exp.	0.85	10
E_{DF}		n/p, drift field, exp.	0.85	10
F	10	n/p, com.	1.78	15
G	10	n/p, com.	1.79	15
H	1	n/p, com.	1.80	15
J_{DF}		n/p, drift field, exp.	2.07	6
K	1	n/p, com.	1.69	15

*com. = commercial, exp. = experimental.
†The active area includes the surface covered by the fine grid lines of the cell and excludes the surface covered by the main grid lines.

Irradiation and Dosimetry

The bombardment of the cells was carried out in the NRL 2-Mev electron Van de Graaff accelerator. This apparatus produces a vertical electron beam which is extracted

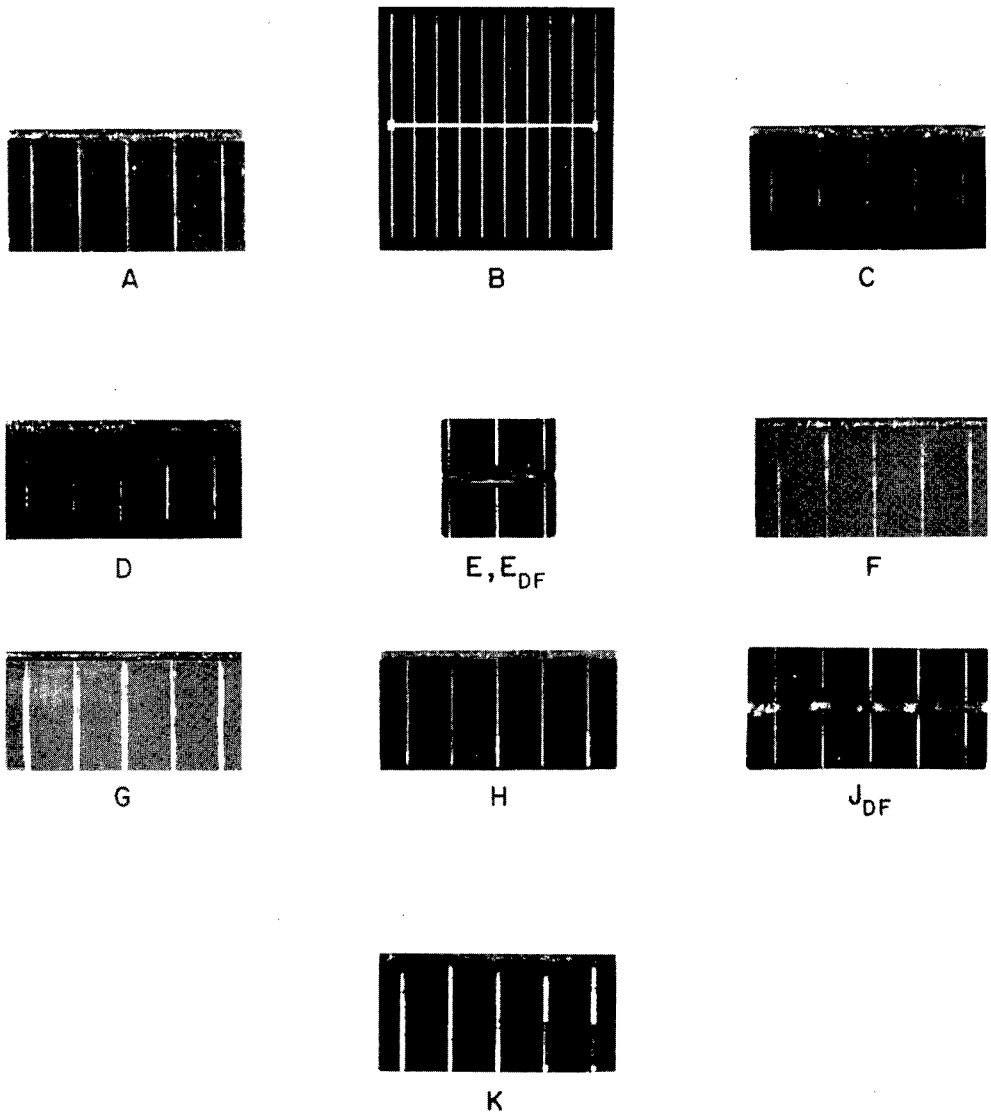

Fig. 2 - Photographs of the ten configurations of solar cells used in this experiment

through a 3-mil aluminum window and scattered through a 6-in. air path. The cumulative scattering effects of the window and air provide a beam spot having a diameter of 2 in. with a maximum intensity variation of 2 percent as measured by a Faraday cup.

To ensure uniformity of integrated electron flux to all solar-cell specimens, they were positioned in appropriate recesses located near the circumference of an aluminum wheel (27.5 in. diameter, 0.19 in. thick) rotating at 10 rpm under the beam tube of the Van de Graaff (Fig. 3). The circular path of each cell was the same, and each passed through the axis of the beam tube about 6 in. below the exit window. The deviation in uniformity of integrated flux from one cell to another did not exceed 0.25 percent at 10^{13} electrons/cm^2 and was much less at the larger doses. The flux level for each bombardment was so chosen as to permit a sufficient number of wheel revolutions to make certain that all cells received the same exposure dose within the aforementioned tolerance. For example, an exposure dose of 10^{13} e/cm^2 required 560 revolutions, whereas 8400 revolutions

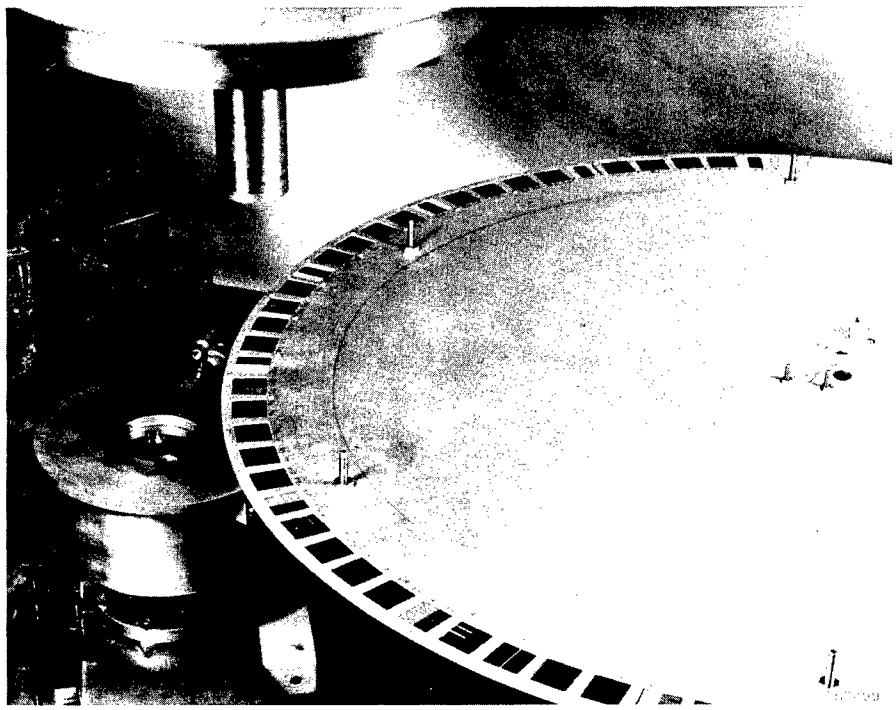

Fig. 3 - Experimental arrangement at the electron Van de Graaff, showing the solar cells in place on the rotating wheel, under the beam tube. The double-aperture Faraday cup is shown in position to monitor electron flux.

were needed for a dose of 10^{16} e/cm^2. Air was continuously blown across the surface of the wheel to cool the cells. As a result, the temperature rise of the cells was no greater than 3°C even during the highest-flux bombardment in the investigation. Temperature measurements were performed by a copper-constantan thermocouple in intimate contact with the wheel surface.

An electron-beam calibration was effected prior to each bombardment by means of a vacuum Faraday cup placed in the center of the beam at the same position the cells would eventually occupy during irradiation. The observed flux was then correlated with the short-circuit current generated in a prebombarded solar cell by exposure to the same flux. The purpose of the prebombardment was to ensure that the diffusion length of the radiation-monitoring cell remained at a virtually constant value. This cell was then mounted near the periphery of the wheel in order that an irradiation duty-cycle value could be determined. For the wheel employed in this investigation, the duty cycle expressed in terms of the integrated flux per revolution referred to the exposure dose at the beam center was 0.05. The flux integration was carried out prior to each irradiation to establish the required exposure time for each flux level. During the bombardment of the specimens, the Faraday cup was positioned near the wheel in order to monitor the flux intensity and stability. Less than 1 percent random fluctuation in the flux was thereby noted. The absolute accuracy of the flux measurement was concluded to be within 5 percent, as inferred from an analysis of diffusion-length measurements carried out on the same cell specimens both at the Bell Telephone Laboratories* and in the present NRL investigation.

*Personal communication from W. Rosenzweig, Bell Telephone Laboratories.

UNCLASSIFIED

Measurement Techniques

Current-Voltage Characteristics – The cells were bombarded in accordance with the irradiation schedule presented in Table 2. Prior to the bombardment, however, and following each incremental dose, the I-V characteristic was obtained for each cell under illumination by a tungsten light source. This light source, the same type of illumination utilized to select the specimen cells for the experiment, consisted of a 300-watt reflector flood bulb carefully calibrated to a color temperature of 2800°K (by means of a Pyro-Eye meter made by Instrument Development Laboratories, Inc.). Thereafter the lamp voltage was regulated to within 0.2 volt by means of an electronic voltage regulator. A heat-absorbing filter comprising a 3-cm thickness of deionized water contained in a methyl methacrylate holder with 0.25-in. walls was interposed in the light path. The light intensity incident on the cell holder was measured by observing the short-circuit current output of a reference solar cell placed in the holder. In order to achieve this purpose, ten n/p solar cells (supplied by Western Electric)* were measured in succession prior to recording the I-V curves of the bombarded solar cells. The light intensity was adjusted as required by the simple expedient of locating the cell holder at a distance from the lamp such that the short-circuit current of the reference solar cells was equivalent to that produced by a sunlight intensity of 100 milliwatts/cm^2.

Table 2
The Number of Cells Irradiated at Successive Steps

Exposure Dose (electrons/cm^2)	Number of Cells Exposed*		
	J_{DF}	E and E_{DF}	All others
0	6	10	15
10^{11}	6	9	14
10^{12}	5	8	13
10^{13}	4	7	12
10^{14}	3	6	11
10^{15}	2	5	10
10^{16}	1	4	9

*Following each increment of bombardment, one cell was withdrawn from each group to be retained for reference.

The I-V characteristics of the irradiated cells were than plotted automatically, on an X-Y recorder, while a continuously variable resistive load was inserted across the solar-cell terminals. The short-circuit current and the open-circuit voltage were measured independently by voltage-to-frequency conversion techniques. The limit of accuracy of the short-circuit-current (I_{sc}) data was ±0.1 ma for all cells in the study, with the exception of those in group B. In this instance, a spurious contact resistance at the cell holder was noted, thereby reducing the accuracy to ±0.3 ma. The above data served as the basis for the calculation of the short-circuit current density and the maximum power output.

Diffusion Length – The effect of an electron bombardment on the bulk minority-carrier diffusion length of the solar cells is a problem of particular interest and importance. It has been suggested (18) that the diffusion length is especially sensitive to radiation damage, and more so than are the I-V characteristics. Another obvious advantage inherent in the

*The cells were calibrated by Mr. L. Slifer of the Goddard Space Flight Center.

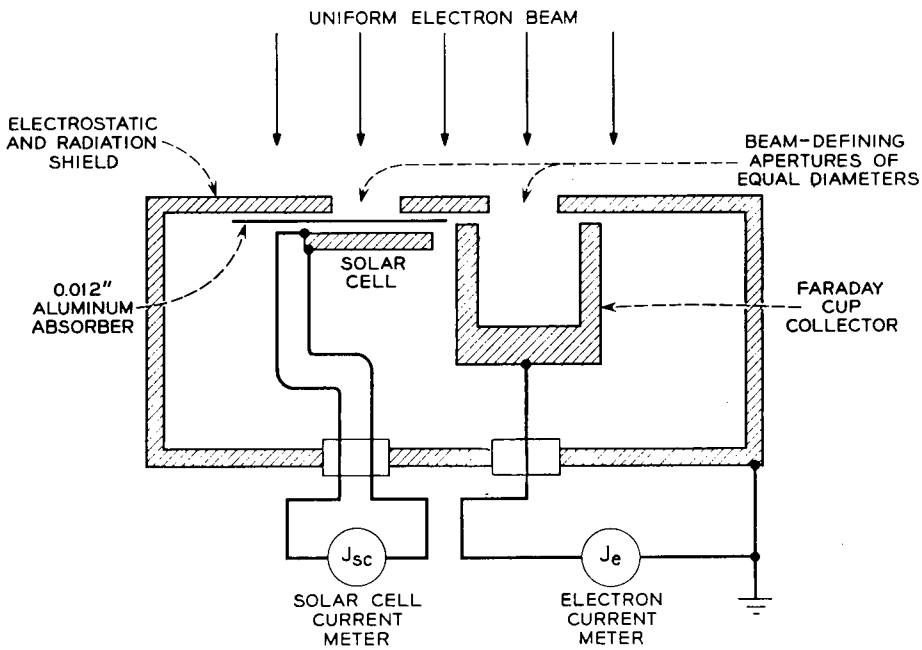

Fig. 4 - Schematic diagram of the vacuum Faraday cup which is used to measure electron flux and minority-carrier diffusion length in the solar cells (14)

diffusion-length measurement is its essential independence of the surface condition of the cell as well as the p-n junction depth, both of which are known to influence the photovoltaic properties of the cell. Although a wide variety of methods are available for the measurement of diffusion lengths in semiconductor junction devices (19), a particular technique referred to as the "electron-injection technique," reported by Rosenzweig (14), has been adopted for the present investigation. The latter method is based on the fact that ionizing radiation may be used to generate excess carriers at a known rate in a p-n junction device. The radiation-generated short-circuit current may then be used to calculate diffusion lengths when the device geometry is known.

In the present application, the electron-injection technique is accomplished by measuring the short-circuit current generated in the cell by a low-intensity 1-Mev electron beam. This was done by mounting the solar-cell specimen within the double-aperture Faraday cup (Fig. 4). The Faraday cup was then centered in the electron beam in order that equal fluxes be incident on both apertures. The inner Faraday cup collected the beam, thereby giving an accurate measure of the flux intensity. The 12-mil aluminum filter placed over the solar cell served to maximize the carrier-generation rate in the silicon. Under these conditions, minority carriers were generated uniformly in the base region of the solar cell. The diffusion length, then, was directly proportional to the number of generated carriers collected at the junction by the relation (14)

$$L = J_{sc}/J_e S_o \tag{10}$$

where

L = diffusion length

J_{sc} = short-circuit current density

S_o = carrier generation rate.

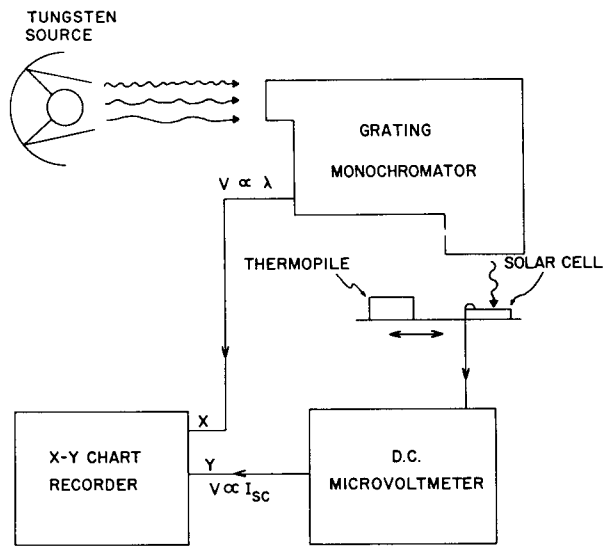

Fig. 5 - Block diagram of the photovoltaic spectral response apparatus

The evaluation of the quantity S_o, carried out in a manner described elsewhere (14), was determined to be 225 pairs per micron for each incident electron.

The diffusion length was measured at the outset of the experiment and following successive bombardments of three cells selected randomly from each of the seven commercial types. The unconventional dimensions and grid arrangements of the experimental cells precluded their accommodation in the special Faraday cup.

Photovoltaic Spectral Response – A third perspective of the radiation damage to solar cells is afforded by an examination of the change in photovoltaic spectral response. This parameter may be generally described as the functional dependence of the solar-cell short-circuit response on the wavelength of incident light. More specifically, the quantum efficiency, a closely related parameter, is defined as the fractional number of liberated minority carriers which diffuse to the junction per incident photon. This fraction is dependent, of course, on the photon energy or wavelength. The general characteristics of the wavelength dependence in a solar cell are well known, exhibiting a falling off of the response at both short and long wavelengths. At short wavelengths, the carrier generation is predominantly localized in the region close to the cell surface. Here the minority-carrier lifetime is extremely short. Hence, the junction collection efficiency for carriers from this region is small. On the other hand, light of longer wavelength generates a substantial number of carriers within the bulk of the cell at a distance exceeding the minority-carrier diffusion length. Once again, the result is a reduction in collection efficiency for these carriers.

In the present experiment, the spectral response of all of the cells for which diffusion length measurements were made was observed. Two of the experimental cells were also included in this study. A modification of the spectral-response apparatus developed at NRL (20) was utilized (Fig. 5). The requirements for the uniform and total illumination of the specimen surface by monochromatic light of relatively high intensity (160 microwatts/cm^2) were satisfied through the use of a Bausch and Lomb grating monochromator. The tungsten-strip lamp source was operated from a voltage supply having a 0.1 percent regulation. In the present instance, since the light beam was not chopped, as is usually done, the short-circuit current response was measured with a Keithley dc microvoltmeter.

Determination of the spectral intensity of the monochromatic light was carried out by the use of a calibrated Eppley thermopile of special design. The response data were plotted automatically as a function of the wavelength by means of an X-Y recorder.

RESULTS

Experimental results will be presented in sufficient detail, so as to reveal many of the small but significant differences in the manifestation of radiation damage in different types of cells. Since much of the data that will be presented are self-explanatory, an extensive discussion of some aspects of the work is unnecessary. Instead, important trends and meaningful conclusions applicable to a type of solar cell will be emphasized.

Current-Voltage Characteristics

An important consequence of the present experiment is that it provides an indication of the degree of nonuniformity existent among solar cells within the same group or class. This is particularly evident when an evaluation is made of the I-V characteristics of the cells, initially as well as following each incremental step of bombardment. The observed inhomogeneity points out the lack of reproducibility involved in all phases of solar-cell fabrication, and especially in the critical process of p-n junction diffusion. It is also evident that variations in the impurity concentration and in the dislocation density in the parent crystal will give rise to inconsistent behavior of p-n junction devices.

The I-V characteristics are presented in Figs. 6 through 16.* The extreme values of this parameter are exhibited for the cell specimens in each commercial group. It is recalled that these cells were selected from a much larger group on the basis of having short-circuit currents closest to the median value of each respective group. Nevertheless, it is noted that in the case of p/n cells, uniformity in the value of I_{sc} does not ensure that the specimens will subsequently degrade in a uniform manner under electron bombardment. Nor does it follow that other electrical parameters, such as the maximum output power or the open-circuit voltage, will be in close agreement. For example, the spread in the values of I_{sc} for unirradiated p/n type cells is ±2 percent, while the corresponding spread in the values of the maximum output power is ±11 percent.

In sharp contrast to the above situation, commercial n/p cells show much less variation in their I-V behavior. However, exceptions are noted in the F and K cells, where two specimens of each group display unexpected and marked deviation in their I_{sc} values after bombardment (Figs. 12 and 16). Since the experimental cells were prepared in smaller lots which required more complex fabrication, they were expected to show less uniformity. In fact, the planar cells (group B) and the specimens in group J are so divergent with respect to their I-V characteristics that only data for a single cell of each type are presented (Figs. 7 and 15).

The short-circuit current densities J_{sc} were obtained from the foregoing data (Figs. 17 through 28). Extreme values for each group are indicated at all levels of bombardment. The values of J_{sc} were computed by dividing the observed values of I_{sc} by the appropriate active area of the cells are given in Table 1. The planar cell area was not conclusively delineated but was determined by noting a difference in the surface reflectivity which was assumed to be the p-n junction intercept on the surface.

It was pointed out previously that I_{sc} was proportional to log L (9,10). From Eq. (8), it follows that

$$L \approx (K\Phi)^{-1/2} . \tag{11}$$

*Figures 6 through 73 are bound consecutively at the end of the text.

UNCLASSIFIED

Then

$$\log L \approx -1/2\ (\log K + \log \Phi) \tag{12}$$

hence

$$I_{sc} \propto (-\log \Phi) \tag{13}$$

The data presented in Figs. 17 through 28 indicate that J_{sc} varies almost linearly with log Φ over two or three decades of integrated flux, depending on the type of cell. Thus, the relation expressed in Eq. (13) is seen to be verified over an extended range of bombardment levels.

It is also noted that the initial current densities of the commercial solar cells fall in the range of 26.5 to 29.0 ma/cm^2. The narrowness of these limits implies that the diffusion and surface-coating technologies have been developed to a high degree. On the other hand, the current densities of the experimental cells are somewhat lower and fall into a range of 21.5 to 26.0 ma/cm^2.

The rates of photovoltaic current degradation may be more easily compared by calculating the percentage of short-circuit current remaining at the conclusion of each bombardment (Figs. 29 through 39). Examination of the linear portions of these graphs reveals that the damage rate for I_{sc} is approximately 20 percent per decade of dose for 1-ohm-cm cells, 15 percent per decade for the 10-ohm-cm and the 25-ohm-cm specimens, and 12 percent per decade for the drift-field type of cell. These values depend on the spectral distribution of the illumination source. The above figures apply to tungsten light illumination and would be about 25 percent less for sunlight measurements (21). However, since most solar-cell measurements are performed under tungsten light, the quoted degradation values constitute a useful and valid basis for making comparative studies.

A summary of the I_{sc} investigation is shown in Fig. 40, wherein is presented the relative order of damage rates for each type of cell. These data facilitate the determination of the integrated flux required to produce a 25-percent decrease in the unirradiated I_{sc} value for each type. The appropriate flux values as well as the flux ratios are listed in Table 3. The flux ratio is obtained by dividing the integrated flux, Φ_c, of 1-Mev electrons required to degrade the short-circuit current of a solar cell to 75 percent of the preirradiation value by the corresponding Φ_c value for the p/n 1-ohm-cm commercial type of cell. Thus the flux ratios for the various kinds of cells indicate the relative radiation resistance. It is evident that the cells may be grouped by polarity and by resistivity. From the point of view of flux ratios, the superiority of all of the n/p cells over the commercial p/n type is clearly established. It is also noted that an increase in resistivity of the bulk material accompanies an increasing resistance to radiation damage in the range of resistivities considered.

A factor of greater significance than the short-circuit current attainable in a solar-cell power system appears to be the amount of power which can be produced following radiation bombardment. Reference to Figs. 6 through 17 shows that the degradation rate of the open-circuit voltage is considerably less than the corresponding decrease in the short-circuit current. In view of the relation expressed in Eq. (5), the power degradation rate will be slightly greater than the current degradation rate. The dependence of the maximum power density on the integrated flux is exhibited in Figs. 41 through 51. The power-damage rate for 1-ohm-cm cells is seen to be 24 percent per decade of integrated flux and approximately 18 percent per decade for the 10-ohm-cm cells, the 25-ohm-cm cells, and the drift-field specimens. In the latter instance, the measurable difference observed in the current damage rates between 10-ohm-cm cells and drift-field cells is compensated by the corresponding open-circuit voltage-damage rates, thereby resulting in very nearly the same power-damage rate. The above results emphasize the need to examine the change in power, or, in some cases, the remaining power output of bombarded cells, rather than to rely on the short-circuit current output as the principal criterion of

Table 3
The Integrated Flux, Φ_c, of 1-Mev Electrons Required to Degrade the Short-Circuit Current of Various Types of Solar Cells to 75 Percent of the Original Value

Cell Type*	Φ_c (e/cm^2)	Flux Ratio
p/n, 1 ohm-cm, com.	1.0×10^{13}	1
n/p, 1 ohm-cm, com.	5.0×10^{14}	50
n/p, 10 ohm-cm, com.	1.0×10^{15}	100
n/p, 25 ohm-cm, exp.	2.0×10^{15}	200
n/p, drift field, exp.	1.5×10^{16}	1500

*com. = commercial, exp. = experimental

Note: The solar-cell current is generated by water-filtered tungsten light with a color temperature of 2800°K. The Φ_c for each type of n/p cell is divided by the Φ_c for the p/n cell and expressed as a flux ratio.

Table 4
The Relative Exposure Dose of 1-Mev Electrons Required to Degrade Certain Types of Solar Cells to Specified Values of J_{sc} and P_{max}

Cell Type	Relative Exposure Dose for the Specified Values of J_{sc} and P_{max}		
	J_{sc} = 19 ma/cm^2	$P_{max}(1)$ = 7 mw/cm^2	$P_{max}(2)$ = 6 mw/cm^2
1 ohm-cm, n/p	40 to 80	20 to 60	27 to 60
10 ohm-cm, n/p	120 and 260	50 and 80	70 and 100
25 ohm-cm, n/p	120	17	20
Drift field, n/p	300	70	100

Note: Relative dose is expressed as a multiple of the dose required to degrade the p/n cells to their respective values.

radiation damage. The results obtained using this criterion for radiation damage are summarized in Table 4, which shows the relative doses required to degrade specific types of solar cells to arbitrarily assigned values of J_{sc} and P_{max}.

Diffusion Length

Minority-carrier diffusion-length measurements for three randomly chosen cells of each commercial type were carried out prior to the first bombardment and following each increment of dose. The observed values are plotted as a function of the integrated flux, as shown in Figs. 52 through 58. The relation expressed in Eq. (12) indicates that a log-log plot of the diffusion length versus the integrated flux should yield a straight line having a slope of -1/2. The predicted theoretical behavior is verified over a limited range of Φ, as evidenced by the data from all of the 1-ohm-cm specimens, whether they are p/n or n/p type. Divergencies from the above value of the slope are noted for both groups of the 10-ohm-cm cells, which reveal a different degradation rate of diffusion length. The significance of these data is that the radiation behavior of the cells of higher electrical resistivity

UNCLASSIFIED

cannot be completely described by the simple relationship expressed in Eq. (7), which is applicable in the case of 1-ohm-cm cells.

An examination of the experimental results from individual cells shows close agreement among the cells comprising each group, with the exception of the F and K groups. Within each of the latter two classes, there is found one cell whose diffusion length following bombardment is significantly different from that observed for the other cells in the group. This result provides confirmation for the conclusions formulated from the I-V characteristics, namely, that the F and K cells are not as consistent in their response to radiation damage as the other types. This abnormality in the measured values of the diffusion length is also illustrated in the photovoltaic spectral response of the cells and will be discussed in more detail in that section. The reason for this type of anomalous behavior is not known at this time.

A summary of the foregoing data is presented in Fig. 59, wherein the linear sections of the diffusion-length degradation curves are exhibited. The results shown for the F and K groups are the average values of the two cells of each type which were in closest agreement. Reference to curves provides support for the conclusions drawn from the I-V characteristics with regard to the order of radiation resistance of the cells. Thus, all of the n/p cells in this study are superior to the p/n cells, from the point of view of retaining long diffusion lengths, and also the 10-ohm-cm cells show less radiation damage than the 1-ohm-cm specimens on the same basis. Furthermore, the ascending order of 1-ohm-cm cells according to the diffusion lengths observed after bombardment is exactly the same as the order with respect to the short-circuit current density, over the range of integrated flux between 10^{14} to 10^{16}e/cm ^{2}, even though the differences are small from one class to the next. It is particularly interesting to note that such differences can be accounted for by small variations in the resistivity of the bulk silicon utilized by different manufacturers.*

It should also be pointed out that the decidedly large differences observed when the diffusion lengths of the F and K groups are compared are not reflected as correspondingly large differences in the short-circuit current densities in the same respective groups. This effect appears to be related to the previous observations made for higher resistivity cells which cannot be characterized by the simple form of Eq. (7).

The dependence of the short-circuit current on the logarithm of the diffusion length alluded to previously (9) is shown in Fig. 60. Although this relationship has been verified only for the case of short-circuit current generated by unfiltered tungsten-light (10), reference to Fig. 60 reveals that the same relationship is satisfied for the water-filtered tungsten light, except for very heavily damaged p/n cells.

A graphical representation of the damage constant K, defined in Eq. (9), is pictured in Fig. 61 for all of the cells for which the diffusion length was measured. The anomalous cells in the F and K groups are clearly distinguishable in view of the fact that they are characterized by damage constants indicative of resistivities grossly different from the group average. The abnormally low values for the damage constant of the cells in group F appear to arise from the unexplained slope of the L vs $\log \Phi$ curve in Fig. 55 and therefore cannot be interpreted in the same light as the damage constants of the other cells.

The empirical relationship between the damage constant and the open-circuit voltage of the unirradiated cell is illustrated in Fig. 62. Since the open-circuit voltage is known to be related to the resistivity of the bulk material, as is shown in Fig. 63, and since it is seen that the K value is also a function of the resistivity, it appears possible to ascertain the value of K for a given cell without the need for performing the bombardment.

*Personal communication from W. Cherry, Goddard Space Flight Center, NASA.

The present study indicates that a good estimate of the value of the damage constant for all cells except those in group K can be obtained by means of the curve plotted in Fig. 62.

Finally, the value of the damage constant for the group D solar cells reported here is within 3 percent of that reported by Rosenzweig (18) and Denney (21). This constitutes a measure of the accuracy of the present flux determination and of the diffusion-length measurements.

Photovoltaic Spectral Response

The relative photovoltaic spectral response was obtained for all solar cells which were included in the diffusion-length measurements. Accordingly, this information is available for verifying the previously observed dissimilarities in diffusion length and short-circuit current between individual cells, as well as for comparing photon conversion efficiencies between various cell types. The measured values of spectral response are utilized in the calculation of the quantum efficiency in the following manner. First, the relative response is normalized on the basis of constant illumination intensity; next, the normalized response is divided by the number of photons represented by the light energy at each wavelength.

The above results are reported in Figs. 64 through 73, wherein the wavelength dependency of percent quantum efficiency of cells characteristic of each type is shown as a function of the integrated flux. Data from only one cell are reported for each group in which there is close agreement with regard to spectral response properties. On the other hand, the response data from two cells of groups F and K, respectively, are presented in view of the marked divergence of results in these groups.

A study of the spectral response curves included in Figs. 64 through 73 makes possible a comparison of the maximum quantum efficiencies, as well as the corresponding wavelengths at which the maxima occur. The wavelength at which the maximum is observed is a function of the junction depth and the surface reflectivity of the solar cell.

Another property which characterizes the effect of bulk-radiation damage on the minority-carrier diffusion length is the well-known decrease in the long-wavelength response of silicon solar cells after electron bombardment. In fact, a qualitative comparison of the diffusion lengths of the two cells in the F group after 10^{16} electrons/cm^2 can be obtained from their respective quantum-efficiency values observed at a wavelength of one micron. Here, the ratio of diffusion lengths is 22 to 12, whereas the ratio of quantum efficiencies is 16 to 9 percent. A further comparison for the two specimens in the K group under the same experimental conditions yields a diffusion-length ratio of 12.5 to 7.2, while the corresponding efficiency ratio is 7 to 4 percent. While these figures are of some interest, they are insufficient to establish a direct relationship between the two quantities. Nor can comparison between cells of different groups be necessarily valid, in view of the fact that the surface reflectivity of a cell has a considerable effect on the value of the quantum efficiency. However, the spectral-response data do indeed appear to confirm the results obtained on silicon solar cells in the other types of measurements summarized above.

CONCLUSIONS

The radiation damage induced in silicon solar cells by 1-Mev electron bombardment has been investigated by utilizing three distinct methods of approach; namely, study of I-V characteristics, diffusion-length measurements, and photovoltaic spectral responses. An analysis of the data shows that each method individually is sufficiently applicatory and sensitive to provide a basis for meangingful comparisons with regard to the radiation

resistance of various cell types. A crosscorrelation of conclusions derived from each experimental technique reveals a high degree of consistency and confirms the accuracy in results as well as the confidence to be placed in the separate analytical methods. Of particular interest is the good agreement between the values of diffusion length and those of the short-circuit current density in the bombarded 1-ohm-cm n/p cells, even though small variations exist in the individual resistivity of the silicon.

While accurate degradation rates of specified characteristics of solar cells are readily established, a definition of radiation resistance or a sensitivity to radiation are not as simple to state for widespread acceptance. Although the individual solar-cell user has a real need to have a single basis for evaluation, many complicating factors enter into the choice of a suitable criterion. One measure of radiation resistance is obtained from a comparison of the values of exposure dose required for various types of cells to degrade either a particular fractional amount or to a specified value of a selected parameter. For example, the percentage change in short-circuit current or the maximum power point can be used as the criterion. Alternatively, an arbitrary value of one particular parameter may be chosen as the basis of comparison. The first approach generally discriminates against very-high-efficiency solar cells, whereas the second method discriminates against experimental cells which do not have good surfaces or optimum electrical design. Additional complications involved in using one standard of radiation resistance arise from particular applications of solar cells, wherein a limit is fixed on the amount of permissible power variation or where operation at a constant voltage across the electrical load is required. Since it is impracticable to combine all of these factors into a single standard, it is deemed necessary to present the results in sufficient detail so that all of the approaches indicated above may be attempted by a further analysis of the data shown in the figures.

The present investigation leads to the conclusion that a consideration of the output power has more validity for the user than does the short-circuit current. Since the I-V characteristics have shown that a uniform predictable relationship does not exist between power change and current change as a function of the cell type or its resistivity, an observation of the variation in the power output cannot be used to compute a corresponding variation in the current, or vice versa. Furthermore, an arbitrary value of power density rather than a percentage degradation in power is proposed as an index of radiation damage, since from the practical standpoint, a satellite must be maintained at some minimum power level to ensure continuous operation. However, even though the former method is adopted as a basis of comparison, the relative radiation resistance of the cells remains a function of a particular power level.

The above argument is embodied in the following specific conclusions:

1. The 1-ohm-cm p/n cell is much less radiation resistant to 1-Mev electron bombardment than any of the n/p types. This is true for all measured characteristics.

2. The 1-ohm-cm n/p groups are extremely uniform with respect to damage rates and are in close conformity with the theoretical relationship between diffusion length and bombardment dose, as expressed in Eq. (7). Whatever deviations are observed appear to be properly correlated with the variation in the bulk resistivity of the cell where higher resistivity is indicative of greater radiation resistance.

3. The use of n/p cells of higher resistivity, up to 10 ohm-cm, results in further improvement of radiation resistance. However, 10-ohm-cm cells do not exhibit close conformity with Eq. (7). The question remains open and provides a basis for further investigation.

4. The relative radiation resistance of the experimental 25-ohm-cm cell as compared with the commercial n/p cells cannot be validly determined on the basis of the

aforementioned radiation damage criteria. For example, a comparison of absolute power output after bombardment is not meaningful because the group E cells are initially much less efficient than the commercial cells. Thus the E cells, while exhibiting a smaller percentage change in power than the commercial cells, have lower output power following the final bombardment. It is essential to note that the degradation rate of the open-circuit voltage is higher for the E cells. This is partially explained by the fact that carrier removal plays a more important role for prolonged bombardments.

5. A comparison of the 25-ohm-cm and drift-field cells, of practically equal initial efficiency and originating from the same manufacturer, shows a decided advantage for the drift-field cell. Further investigation pointing to a wider application of the drift-field principle to silicon solar-cell fabrication is well justified.

6. In view of the dissimilar radiation behavior of cells with reportedly the same characteristics, it is evident that the use of very few samples as representative of a given type of cell in an evaluation of radiation damage is not a recommended practice. The inclusion of four to six specimens chosen at random from a particular lot appears to be a minimum requirement to ensure that a representative sampling is obtained for the average radiation-damage characteristics of that group.

ACKNOWLEDGMENTS

The author wishes to thank Messrs. W. Cherry and M. Schach of Goddard Space Flight Center, NASA, for suggesting this experiment and supplying the solar cells. The calibrated standard solar cells and tungsten lamps were furnished by Mr. L. Slifer of GSFC. Thanks are due Dr. W. Rosenzweig, Bell Telephone Laboratories, for many helpful discussions concerning dosimetry and diffusion-length measurements. The author is particularly grateful to his colleagues who assisted in this study: Mr. E.L. Brancato for consultation; Mr. J.F. Weller for valuable assistance in the bombardments, diffusion length measurements, and data reduction; Mr. R.J. Lambert for the quantum efficiency measurements and calculations; Mr. M.E. Sharp for the design and construction of much of the apparatus; and Dr. B.J. Faraday for his critical review of the manuscript.

UNCLASSIFIED

REFERENCES

1. Van Allen, J.A., McIlwain, C.E., and Ludwig, G.H., J. Geophys. Res. 64:271 (1959)
2. McIlwain, C.E., Science 142:355 (1963)
3. Hess, W.N., Intern. Sci. and Technol. 21:40 (Sept. 1963)
4. Mandelkorn, J., "A New Radiation-Resistant High-Efficiency Solar Cell," USASRDL Tech. Rept. 2162, Oct. 1960
5. Weller, J.F., "Proton Damage to Silicon Solar Cells" Report of NRL Progress, pp. 1-6, Jan. 1963
6. Hess, W.N., J. Geophys. Res. 68:667 (1963)
7. Braunstein, R., Moore, A.R., and Herman, F., Phys. Rev. 109:695 (1958)
8. Van der Ziel, A., "Solid State Physical Electronics," Englewood Cliffs, N.J.:Prentice-Hall, 1957
   a. p. 381
   b. p. 383
9. Kleinman, D.A., Bell System Tech. J. 40:85 (1961)
10. Denney, J.M., Downing, R.G., Kirkpatrick, M.E., Simon, G.W., and Van Atta, W.K., "Charged Particle Radiation Damage in Semi-conductors, IV: High Energy Proton Radiation Damage in Solar Cells," Space Technology Lab. Report MR-27, 8653-6017-KU-000, Contract NAS 5-1851, Jan. 20, 1963
11. Shockley, W., in "Electrons and Holes in Semiconductors," New York:Van Nostrand, p. 314, 1950
12. Smith, K.D., Gummel, H.K., Bode, J.D., Cuttriss, D.B., Nielsen, R.J., and Rosenzweig, W., Bell System Tech, J. 42(4):1765 (July 1963)
13. McKay, K.G., Phys. Rev. 84:829 (1951)
14. Rosenzweig, W., Bell System Tech. J. 41:1573 (1962)
15. Loferski, J.J., and Rappaport, P., Phys. Rev. 111:432 (1958)
16. Dienes, G.J., and Vineyard, G.H., in "Radiation Effects in Solids," New York:Interscience, p. 13, 1957
17. Loferski, J.J., J. Appl. Phys. 29:35 (1958)
18. Rosenzweig, W., Gummel, H.K., and Smits, F.M., Bell System Tech. J. 42:399 (1963)
19. Bemski, G., Proc. IRE 46:990 (1958)
20. Flesch, J., and Statler, R.L., "Thermal Mechanical and Environmental Characteristics," Report of NRL Progress, p. 31, June 1962
21. Denney, J.M., Downing, R.G., Hoffnung, W.I., and Van Atta, W.K., "Charged Particle Radiation Damage in Semiconductors, V: Effect of 1 Mev Electron Bombardment on Solar Cells," Space Technology Lab. Report MR-28, 8653-6018-KU-000, Contract NAS 5-1851, Feb. 11, 1963

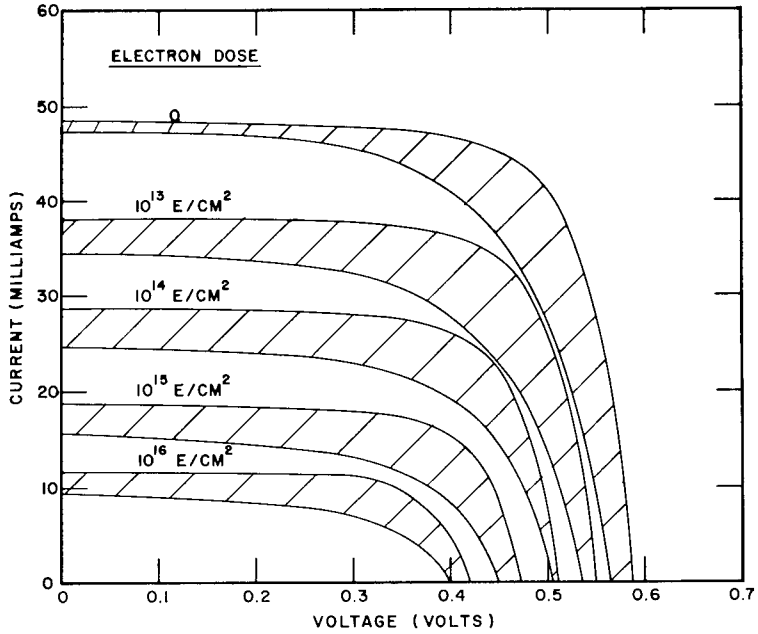

Fig. 6 - I-V characteristic of group A solar cells as a function of electron dose. The widths of the bands illustrate the limits of variation observed in individual cells.

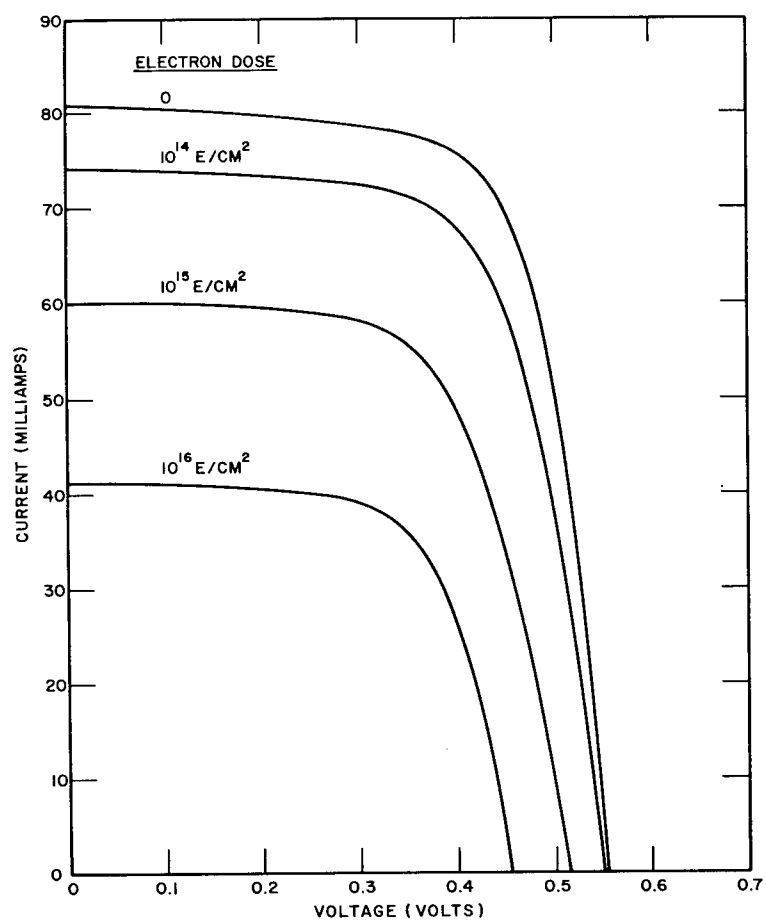

Fig. 7 - I-V characteristic of a representative group B solar cell

UNCLASSIFIED

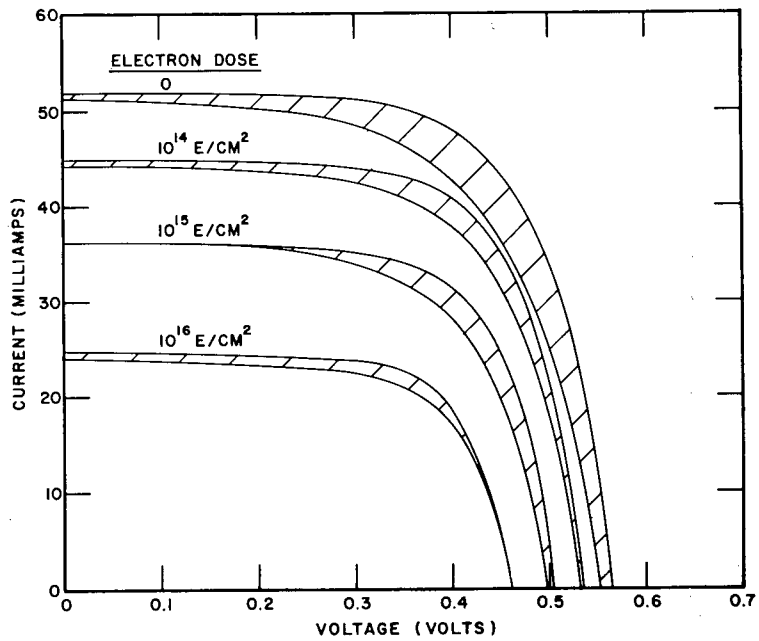

Fig. 8 - I-V characteristic of group C solar cells

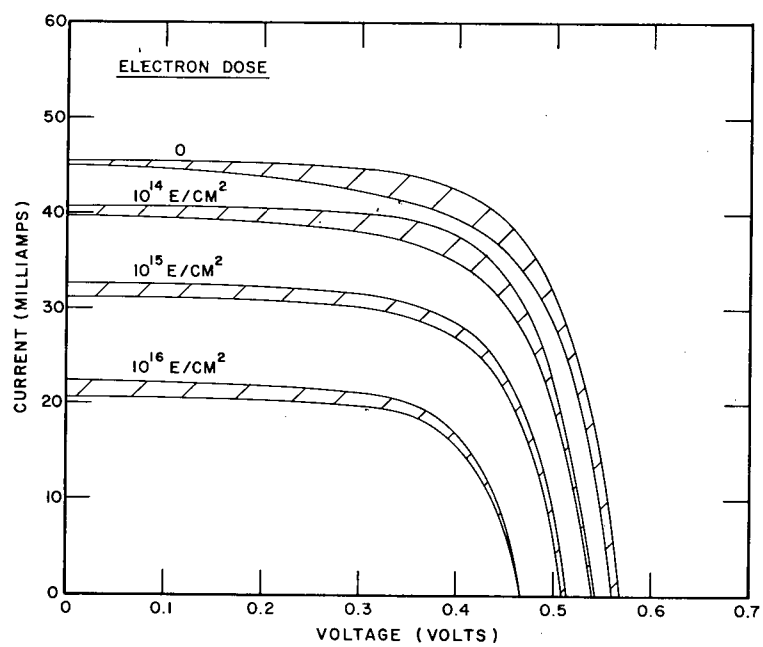

Fig. 9 - I-V characteristic of group D solar cells

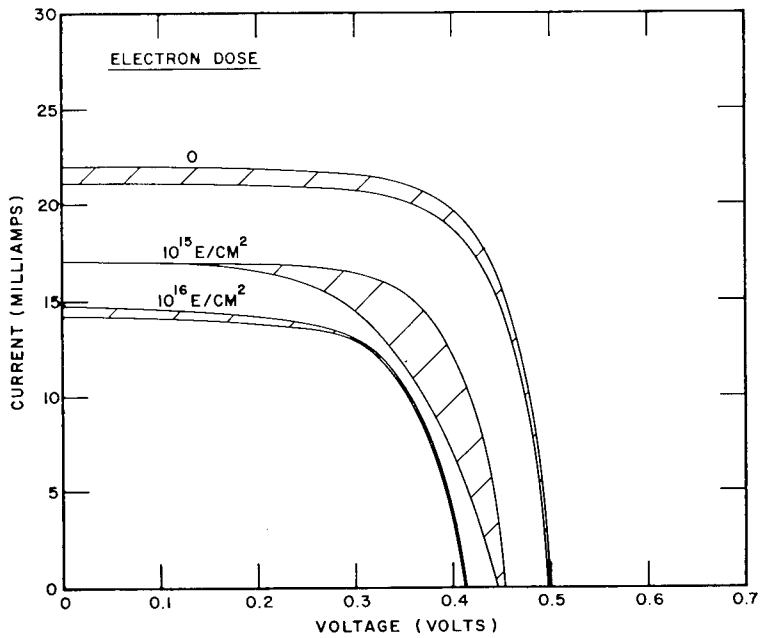

Fig. 10 - I-V characteristic of group E solar cells

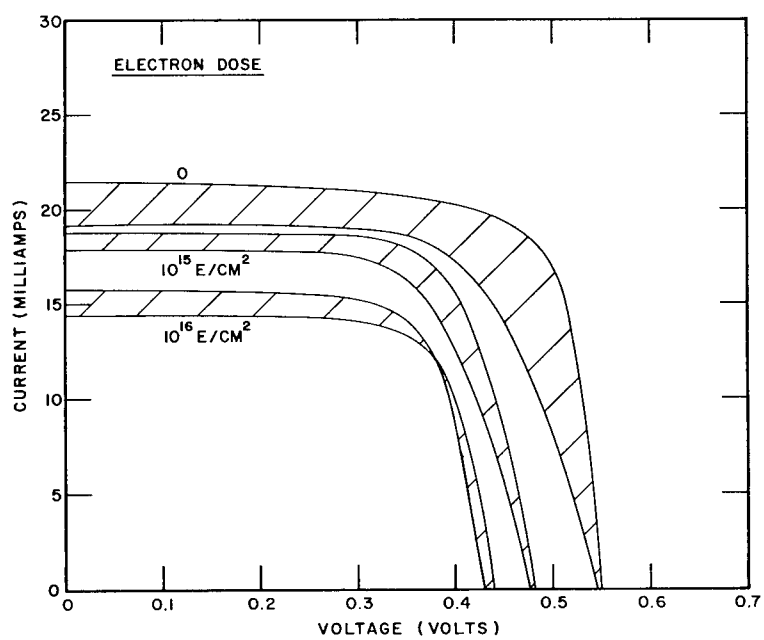

Fig. 11 - I-V characteristic of group E_{DF} solar cells

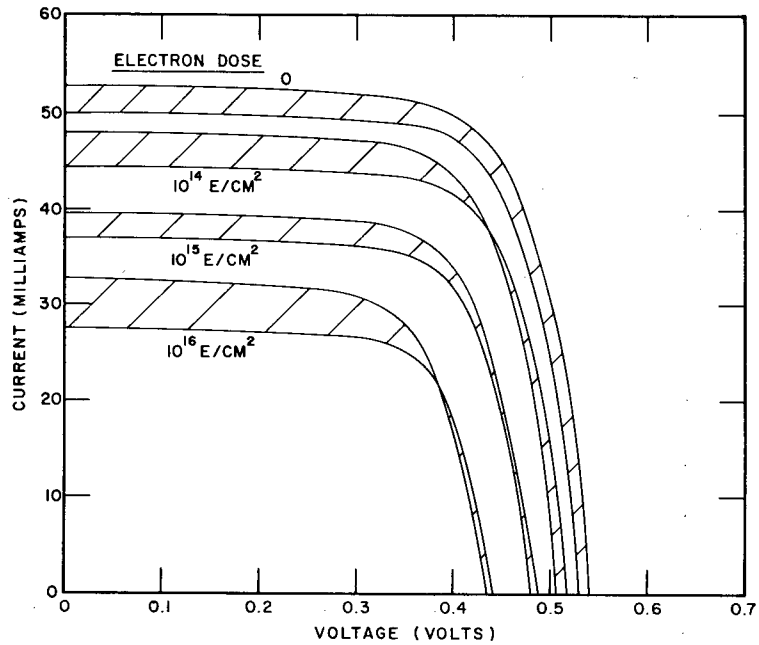

Fig. 12 - I-V characteristic of group F solar cells

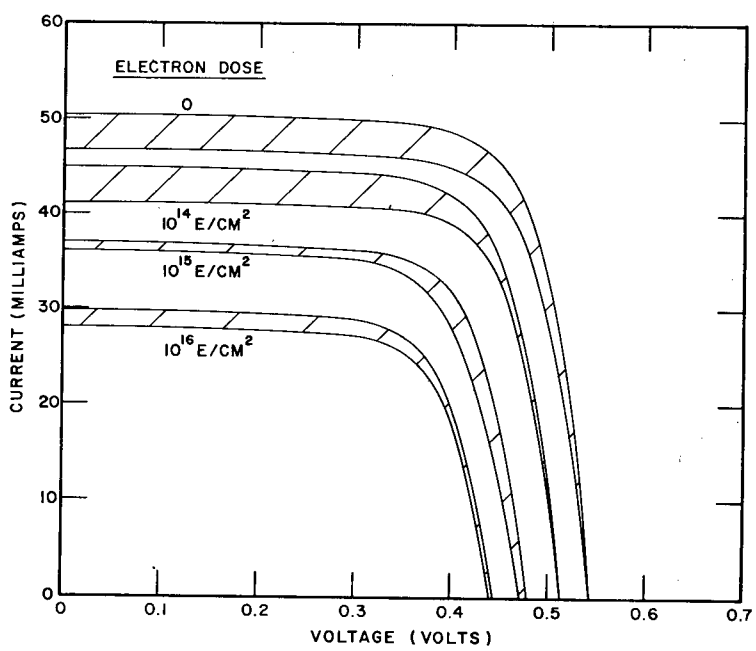

Fig. 13 - I-V characteristic of group G solar cells

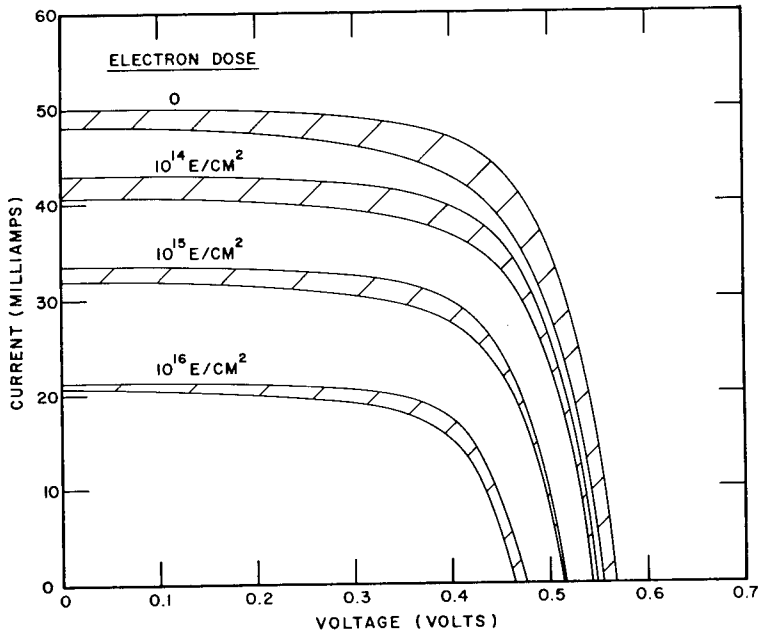

Fig. 14 - I-V characteristic of group H solar cells

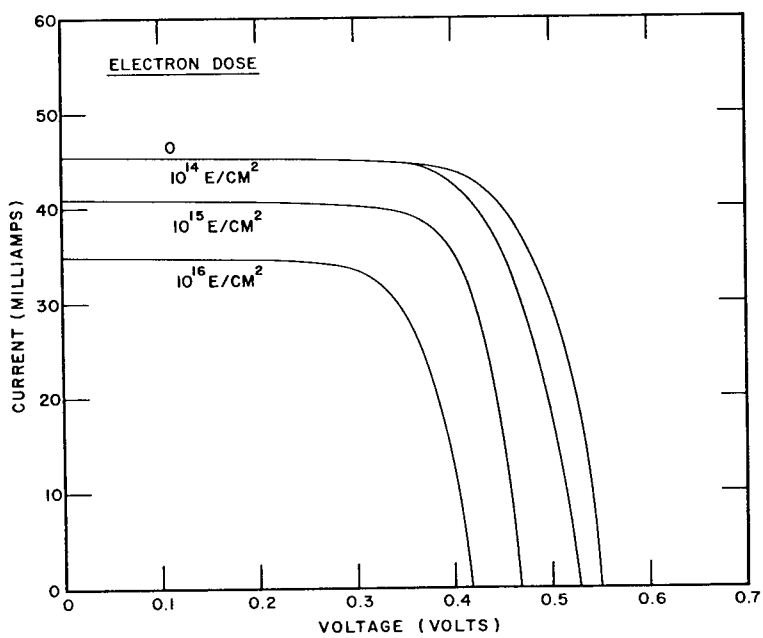

Fig. 15 - I-V characteristic of a representative group J_{DF} solar cell

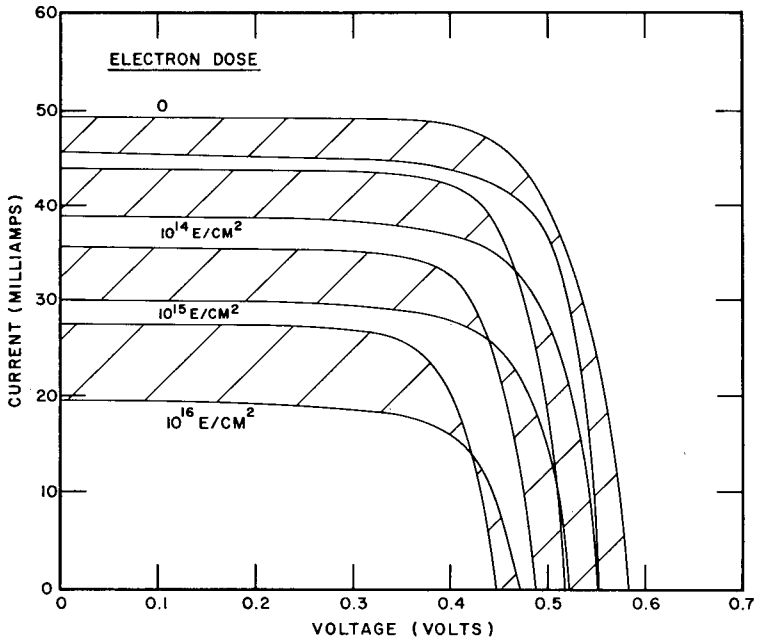

Fig. 16 - I-V characteristic of group K solar cells

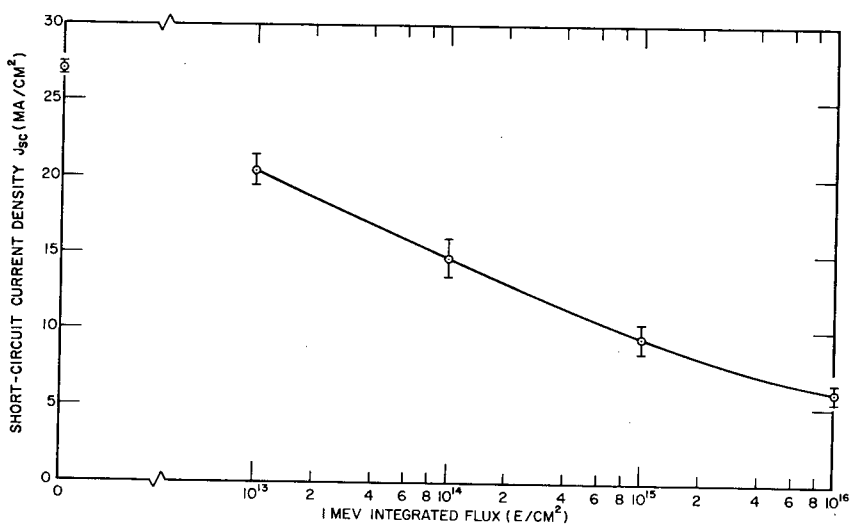

Fig. 17 - Short-circuit current density J_{sc} of group A solar cells after electron bombardment. The median and extreme values are shown.

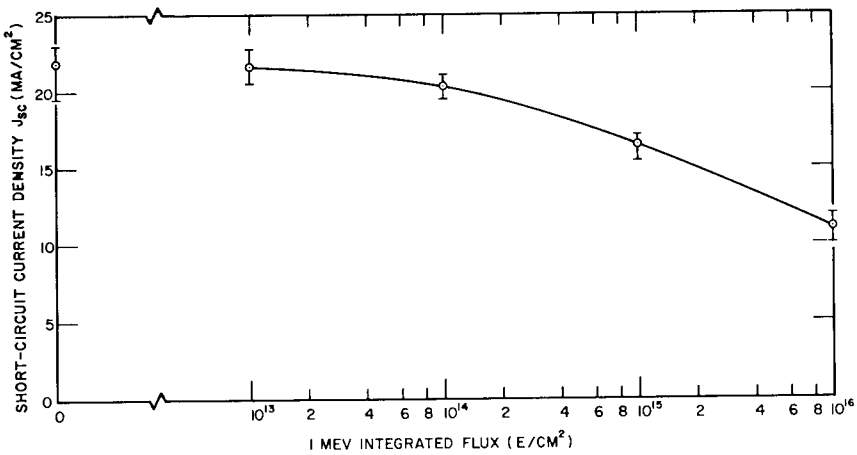

Fig. 18 - Short-circuit current density J_{sc} of group B solar cells

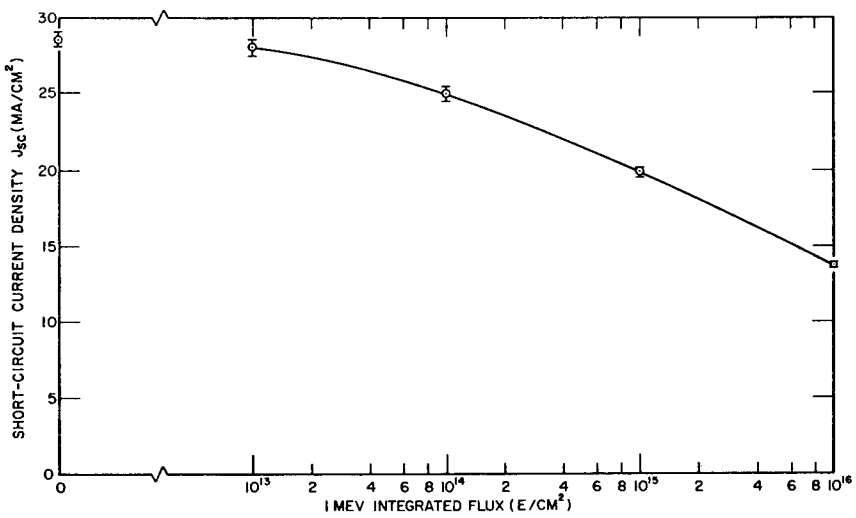

Fig. 19 - Short-circuit current density J_{sc} of group C solar cells

Fig. 20 - Short-circuit current density J_{sc} of group D solar cells

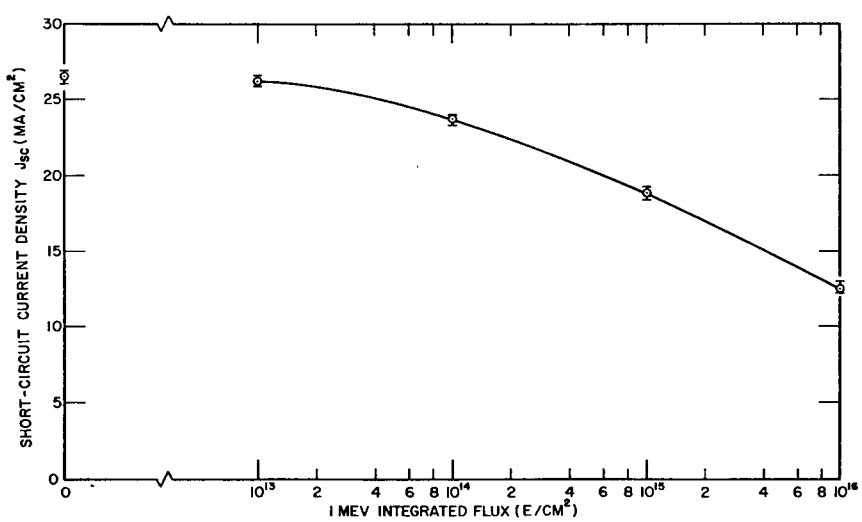

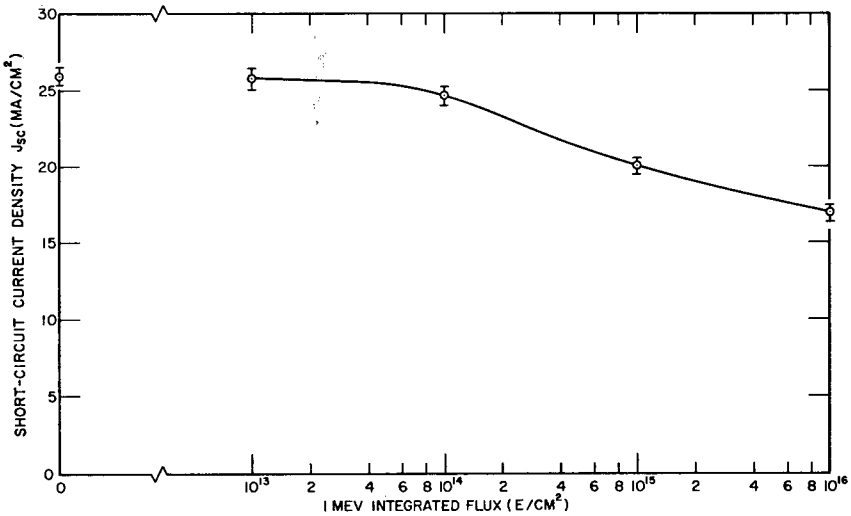

Fig. 21 - Short-circuit current density J_{sc} of group E solar cells

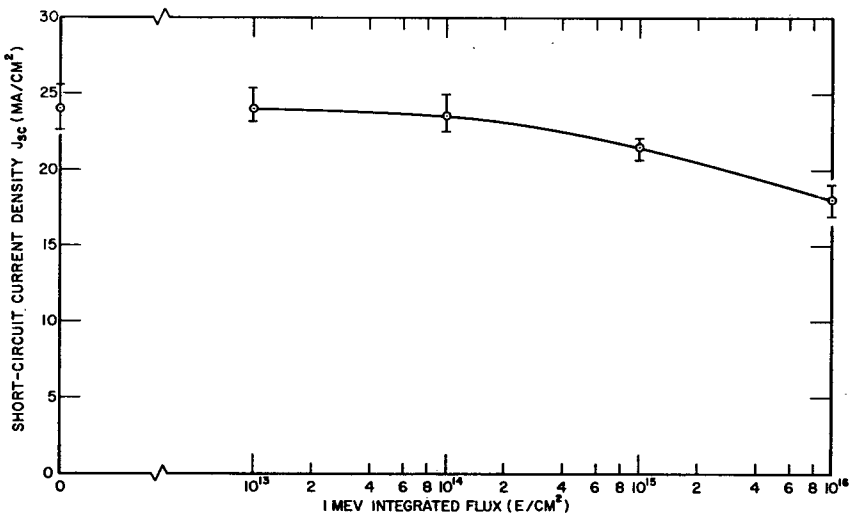

Fig. 22 - Short-circuit current density J_{sc} of group E_{DF} solar cells

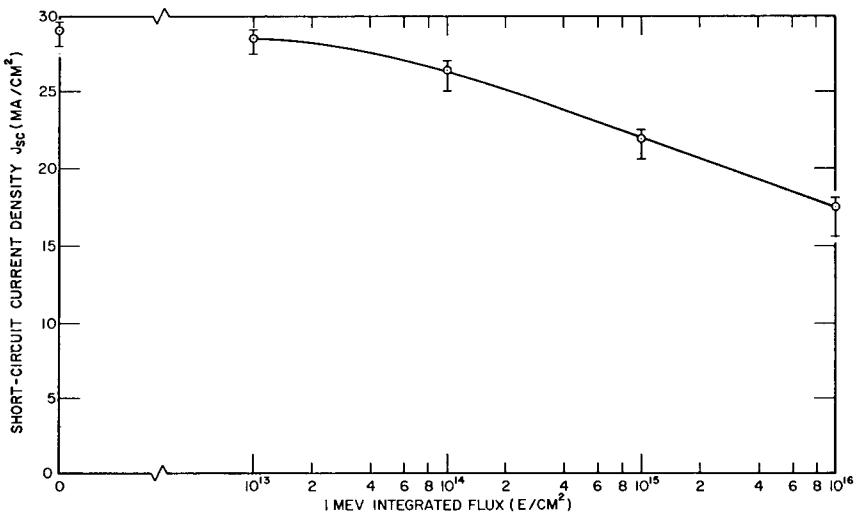

Fig. 23 - Short-circuit current density J_{sc} of group F solar cells

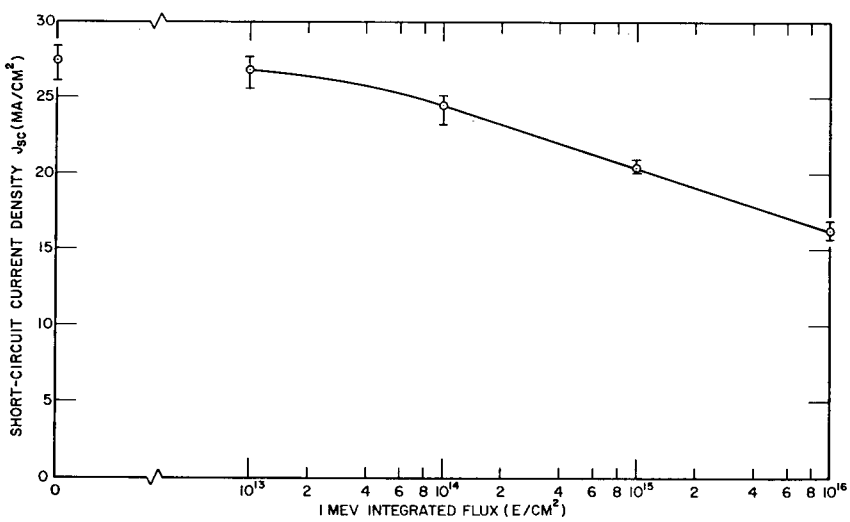

Fig. 24 - Short-circuit current density J_{sc} of group G solar cells

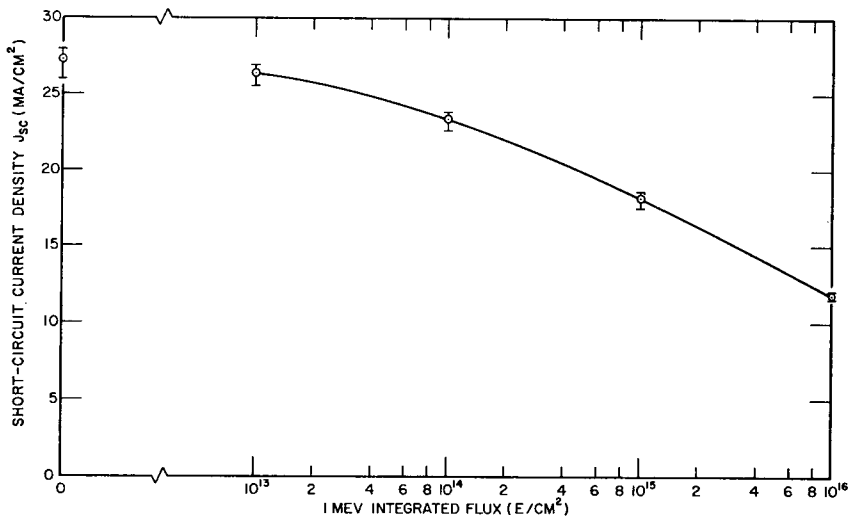

Fig. 25 - Short-circuit current density J_{sc} of group H solar cells

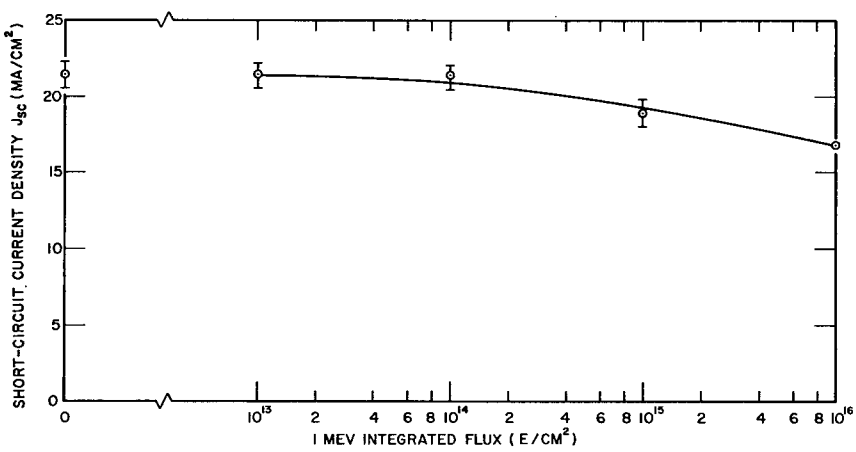

Fig. 26 - Short-circuit current density J_{sc} of group J_{DF} solar cells

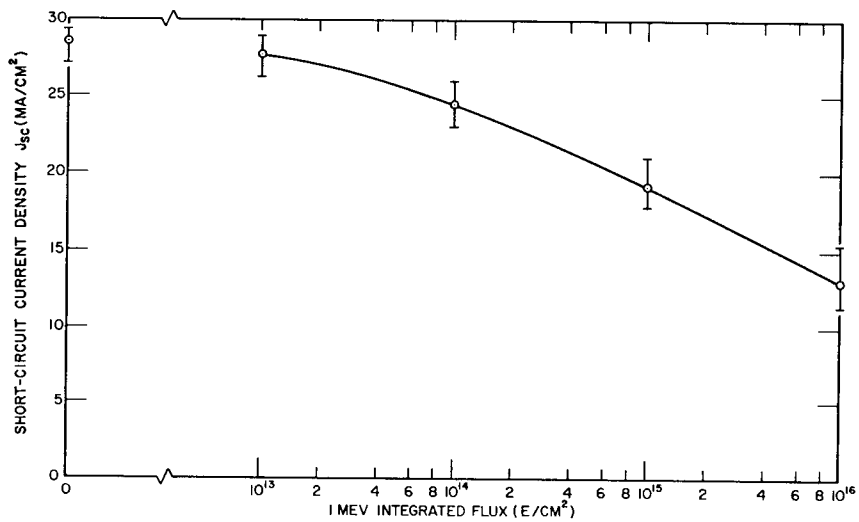

Fig. 27 - Short-circuit current density J_{sc} of group K solar cells

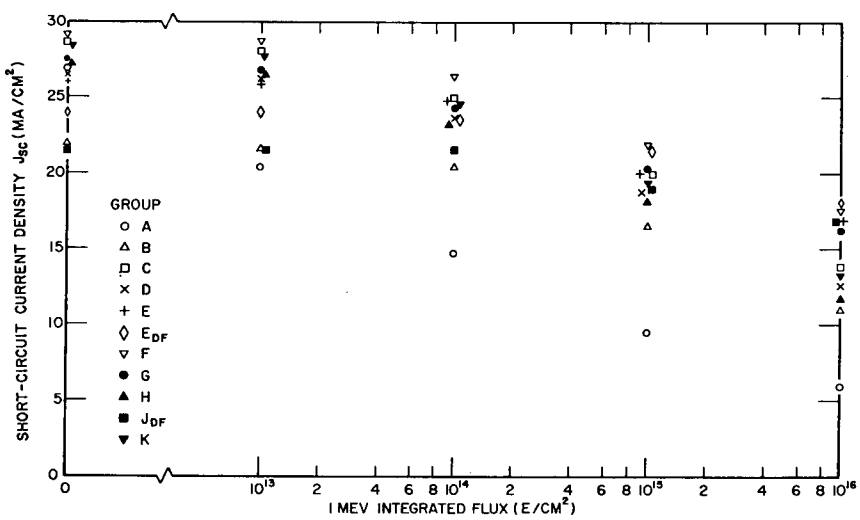

Fig. 28 - Summary of short-circuit current densities of solar cells after electron bombardment

UNCLASSIFIED

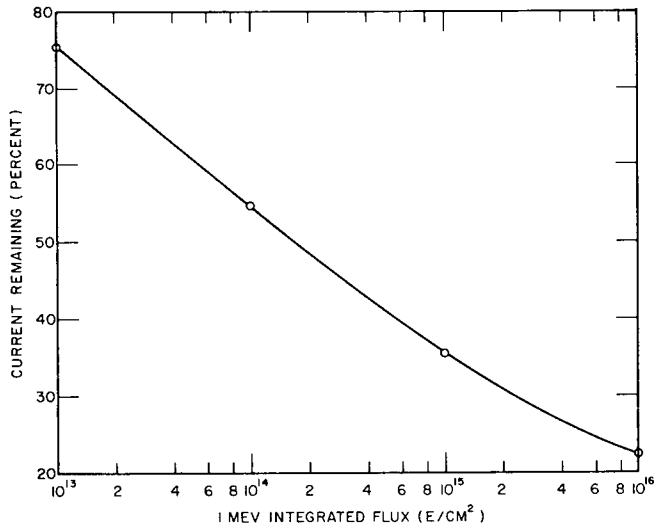

Fig. 29 - Percentage change in short-circuit current of group A solar cells

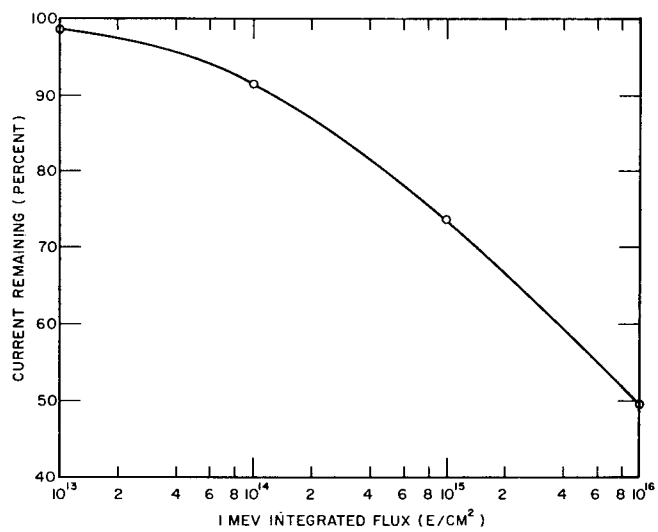

Fig. 30 - Percentage change in short-circuit current of group B solar cells

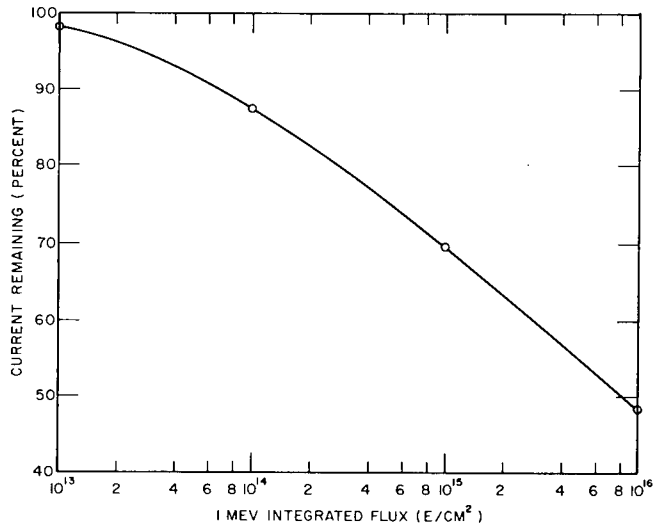

Fig. 31 - Percentage change in short-circuit current of group C solar cells

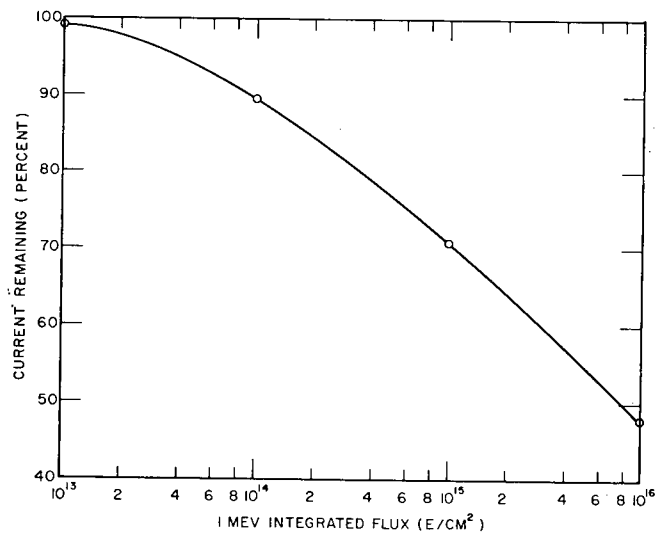

Fig. 32 - Percentage change in short-circuit current of group D solar cells

UNCLASSIFIED

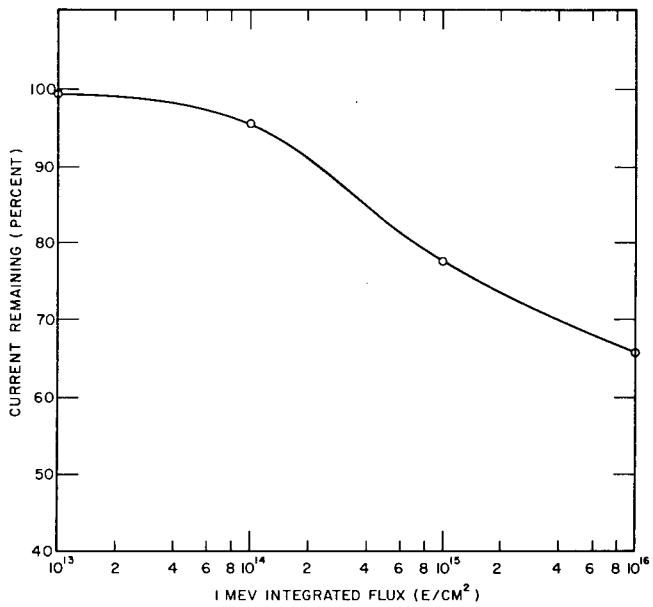

Fig. 33 - Percentage change in short-circuit current of group E solar cells

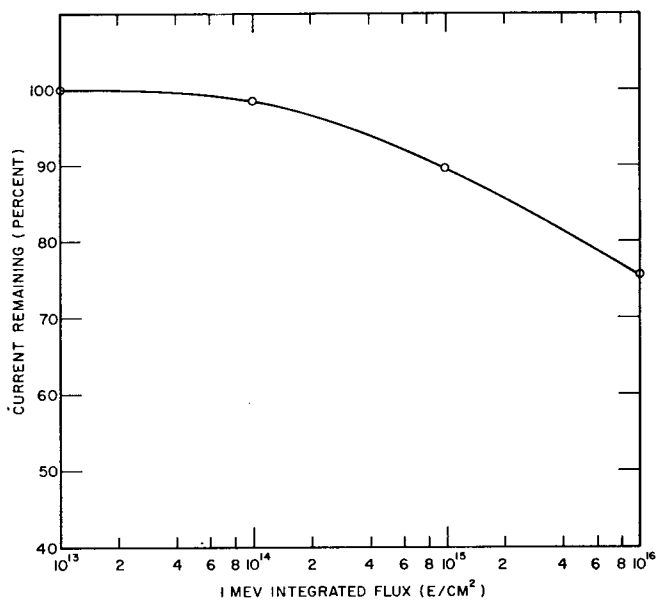

Fig. 34 - Percentage change in short-circuit current of group E_{DF} solar cells

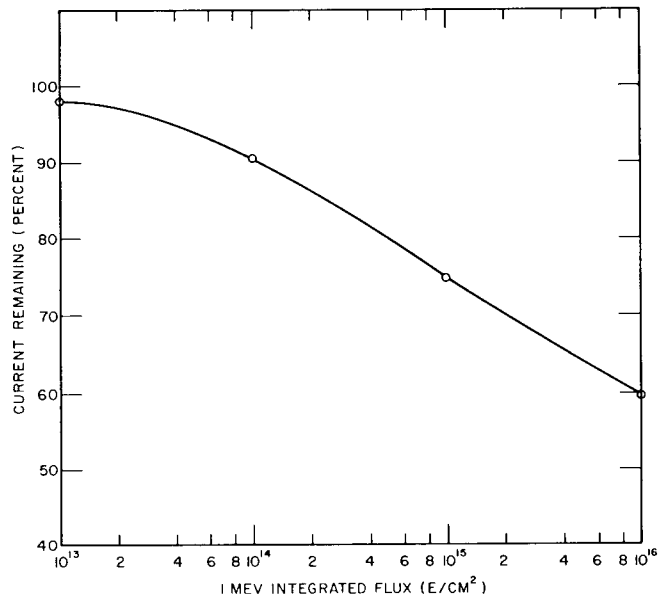

Fig. 35 - Percentage change in short-circuit current of group F solar cells

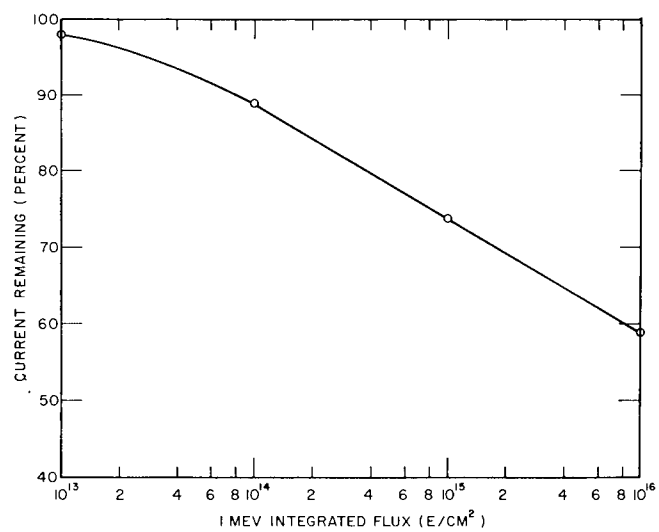

Fig. 36 - Percentage change in short-circuit current of group G solar cells

UNCLASSIFIED

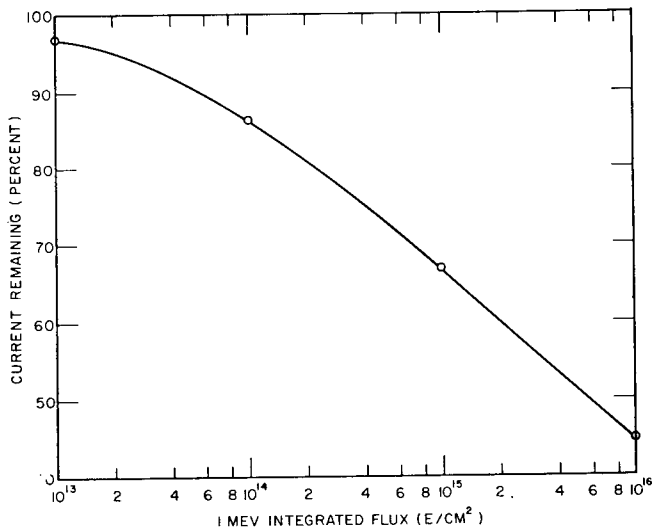

Fig. 37 - Percentage change in short-circuit current of group H solar cells

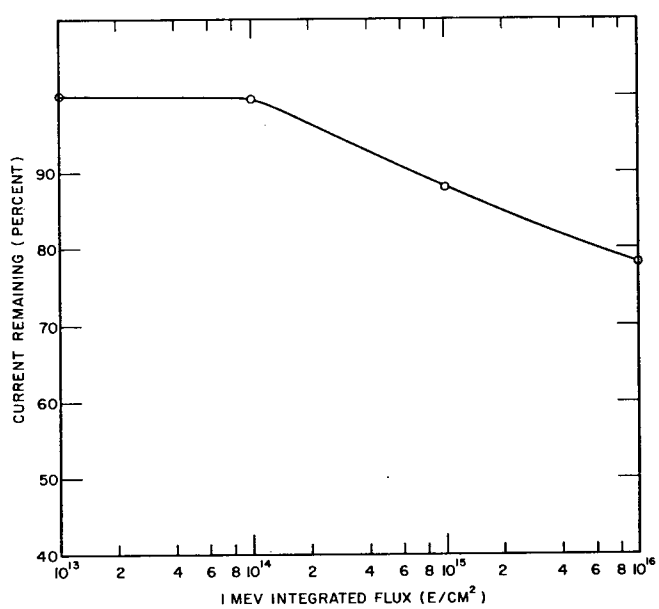

Fig. 38 - Percentage change in short-circuit current of group J_{DF} solar cells

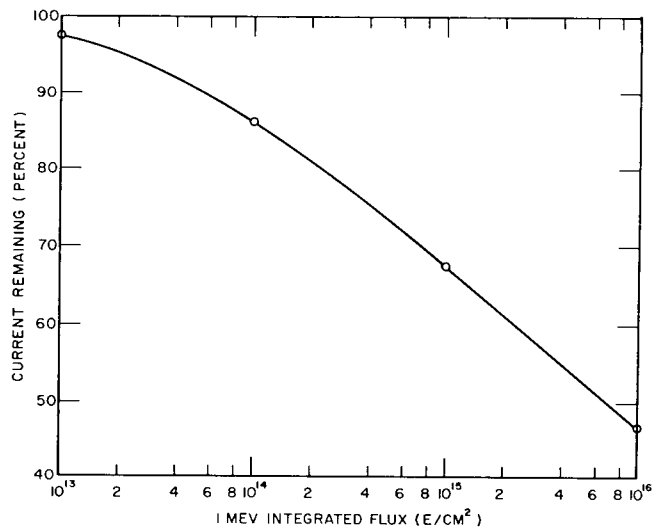

Fig. 39 - Percentage change in short-circuit current of group K solar cells

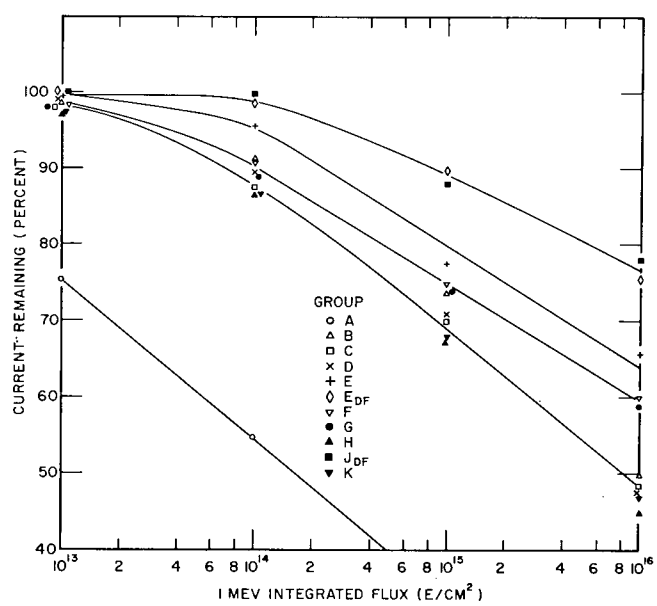

Fig. 40 - Summary of percentage change in short-circuit current of solar cells after electron bombardment

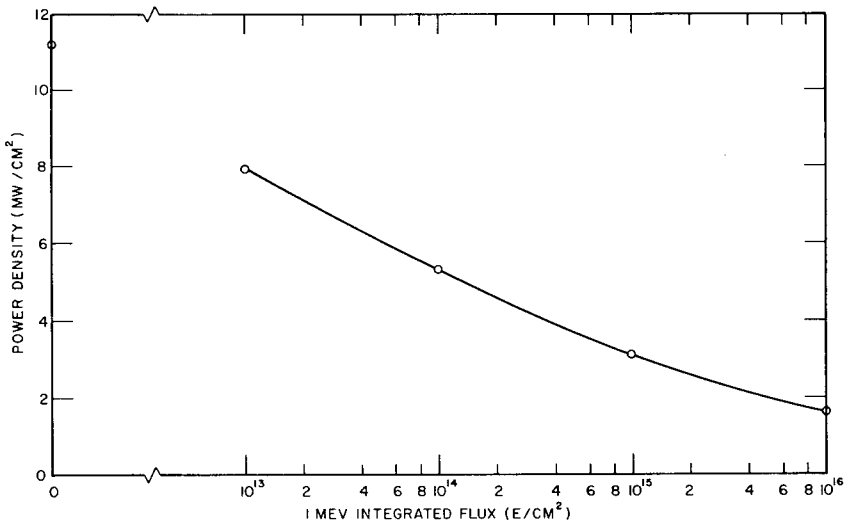

Fig. 41 - Maximum power density of group A solar cells

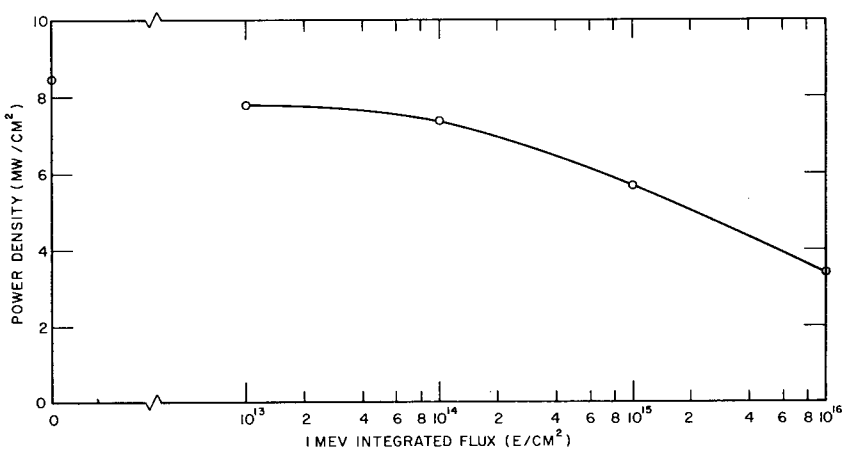

Fig. 42 - Maximum power density of group B solar cells

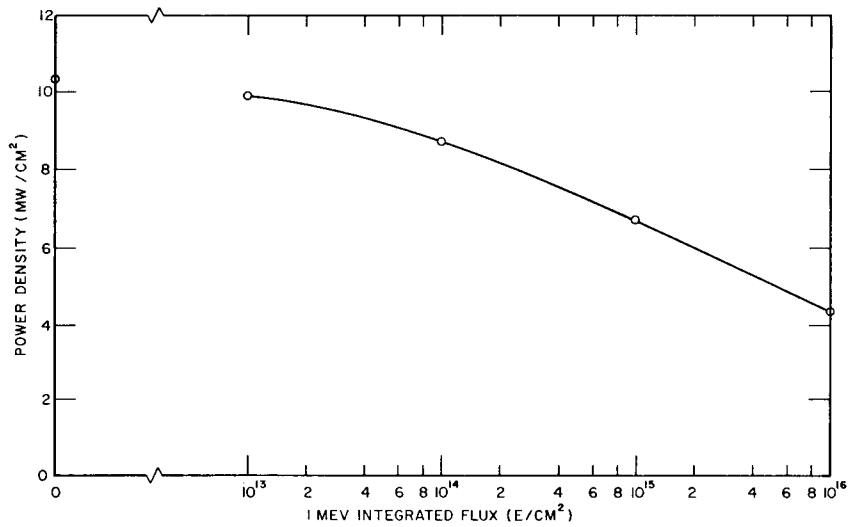

Fig. 43 - Maximum power density of group C solar cells

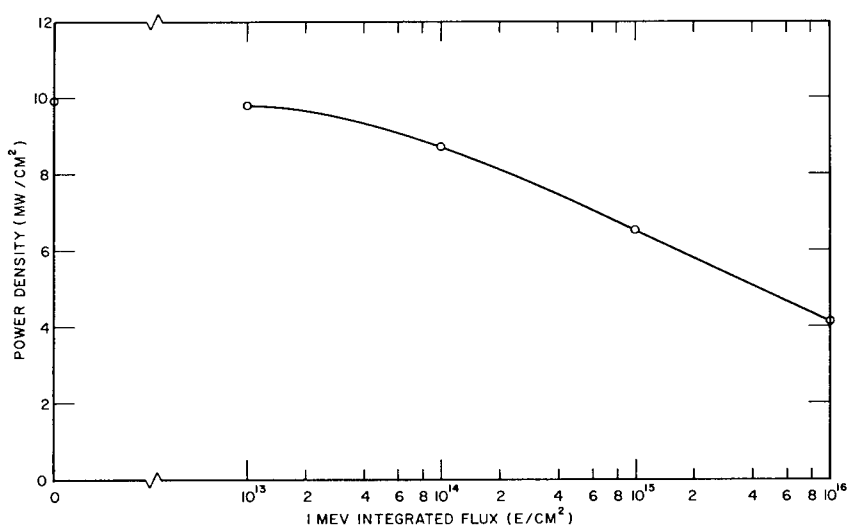

Fig. 44 - Maximum power density of group D solar cells

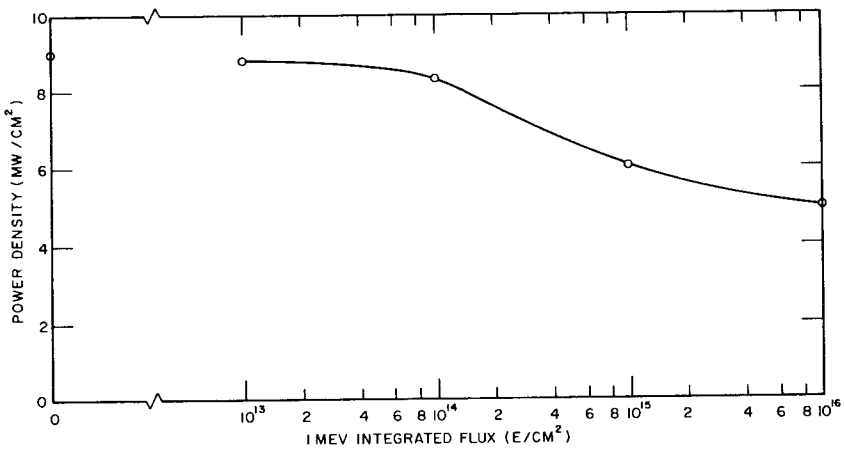

Fig. 45 - Maximum power density of group E solar cells

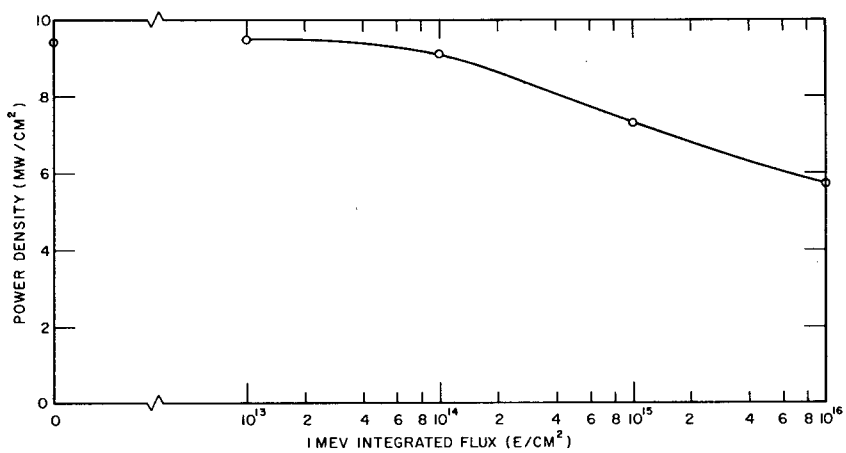

Fig. 46 - Maximum power density of group E_{DF} solar cells

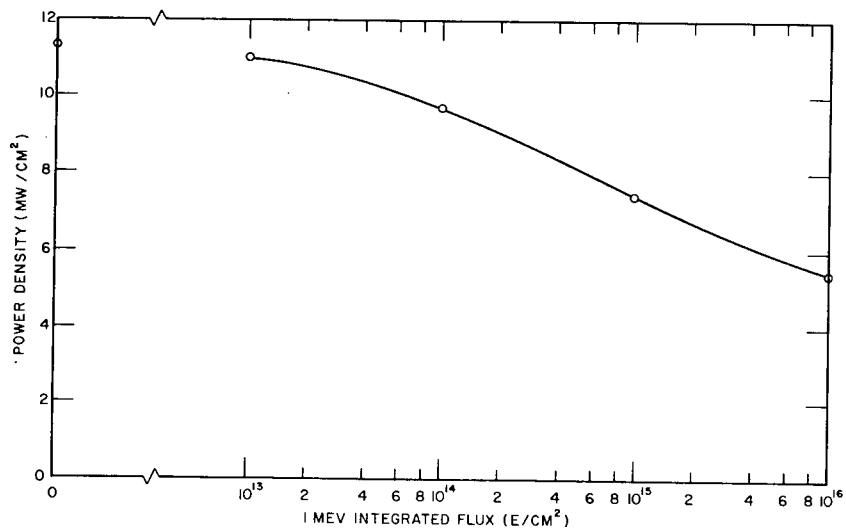

Fig. 47 - Maximum power density of group F solar cells

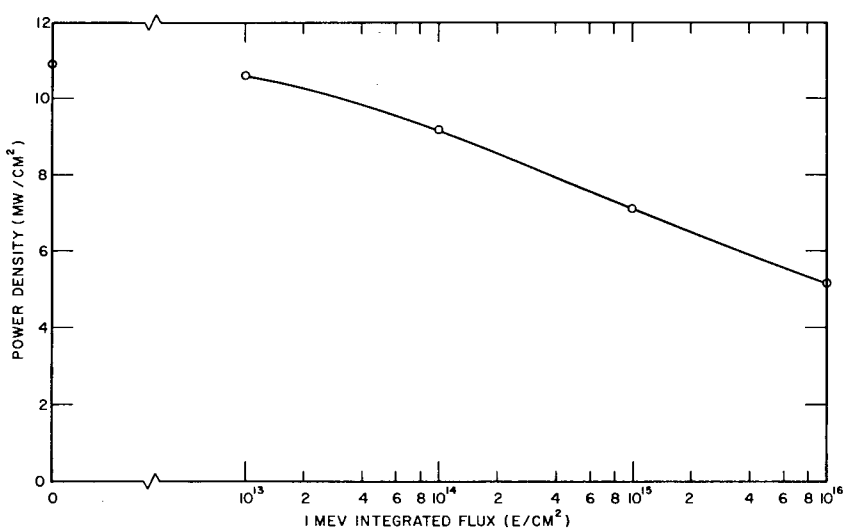

Fig. 48 - Maximum power density of group G solar cells

UNCLASSIFIED

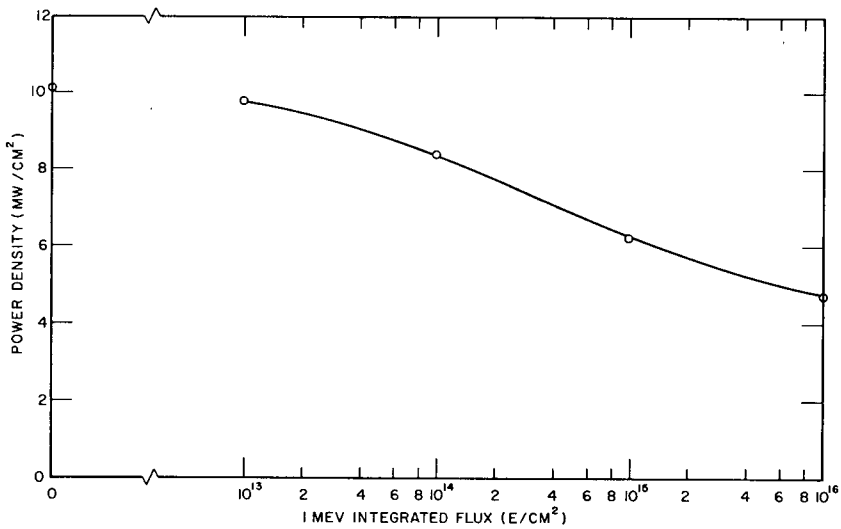

Fig. 49 - Maximum power density of group H solar cells

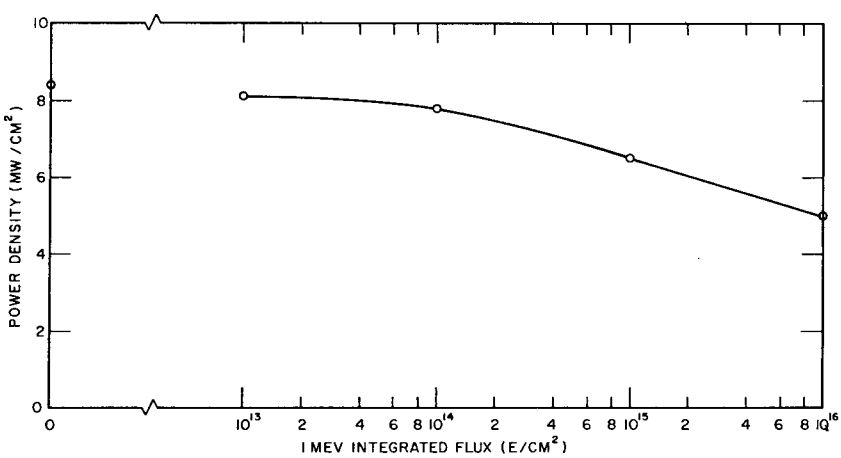

Fig. 50 - Maximum power density of group J_{DF} solar cells

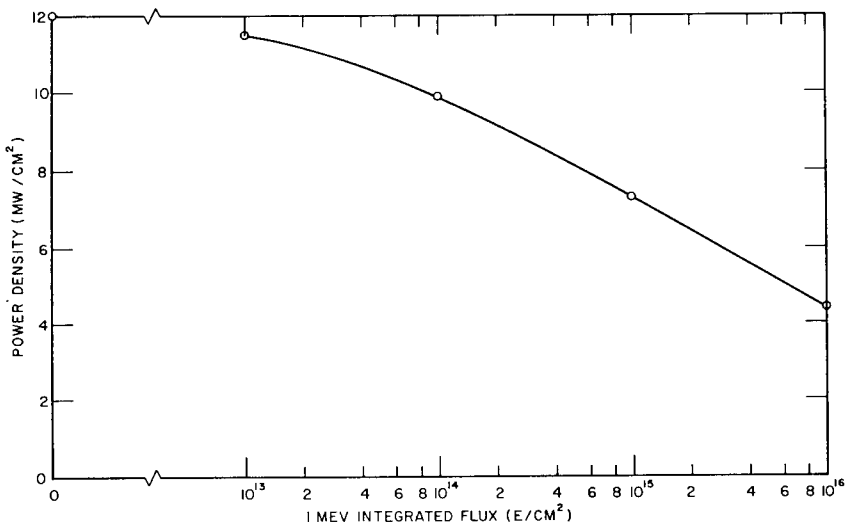

Fig. 51 - Maximum power density of group K solar cells

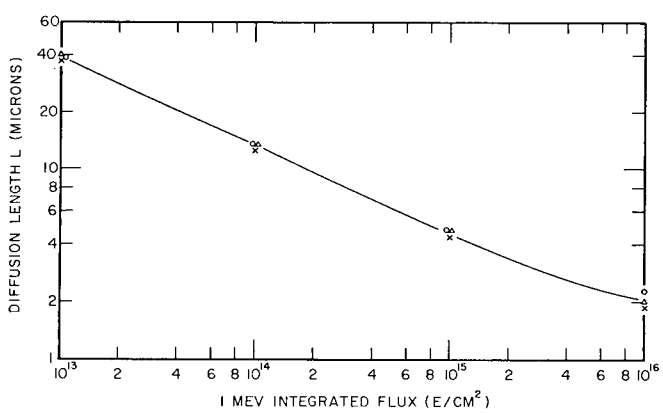

Fig. 52 - Minority-carrier diffusion length L of group A solar cells

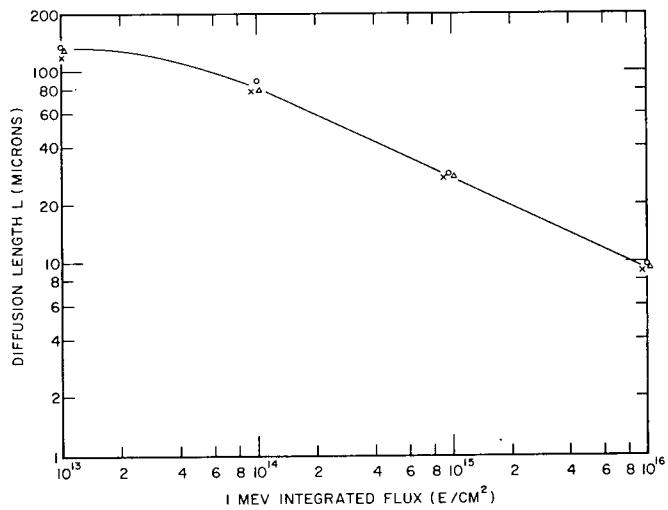

Fig. 53 - Minority-carrier diffusion length L of group C solar cells

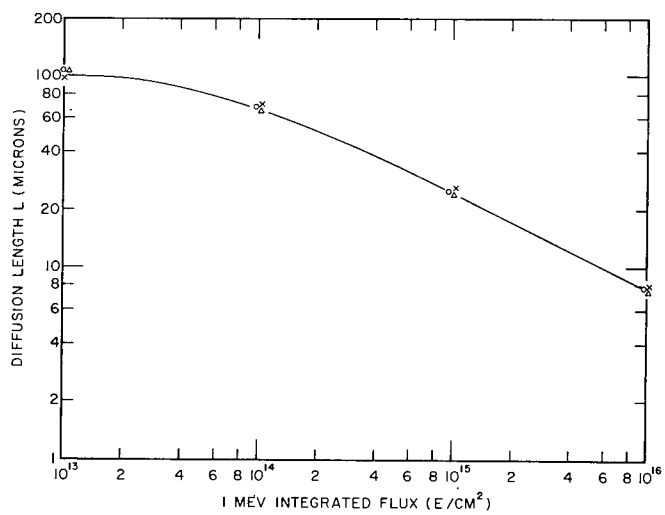

Fig. 54 - Minority-carrier diffusion length L of group D solar cells

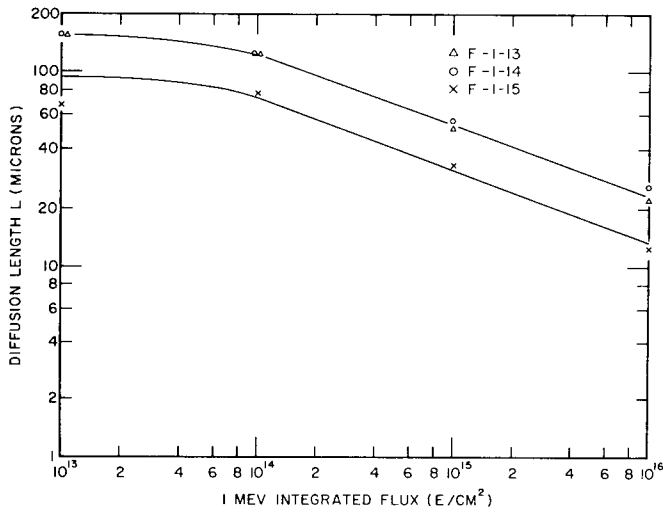

Fig. 55 - Minority-carrier diffusion length L of group F solar cells

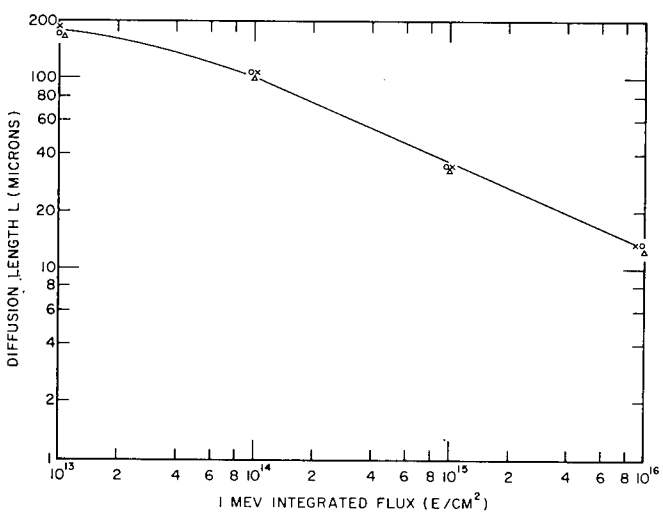

Fig. 56 - Minority-carrier diffusion length L of group G solar cells

UNCLASSIFIED

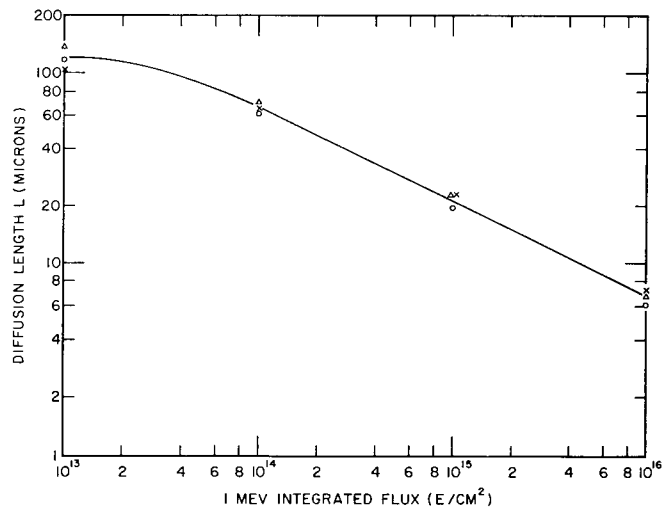

Fig. 57 - Minority-carrier diffusion length L of group H solar cells

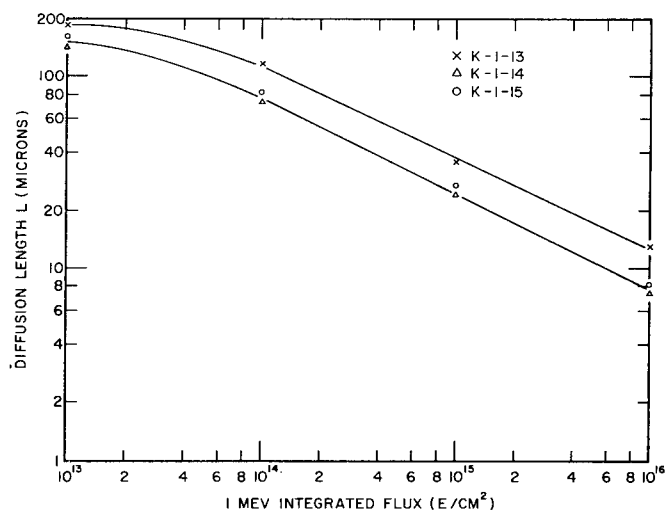

Fig. 58 - Minority-carrier diffusion length L of group K solar cells

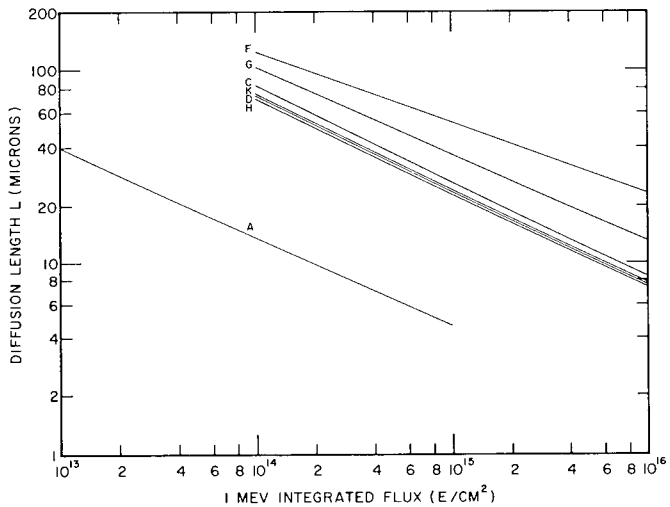

Fig. 59 - Summary of solar cell diffusion-length degradation

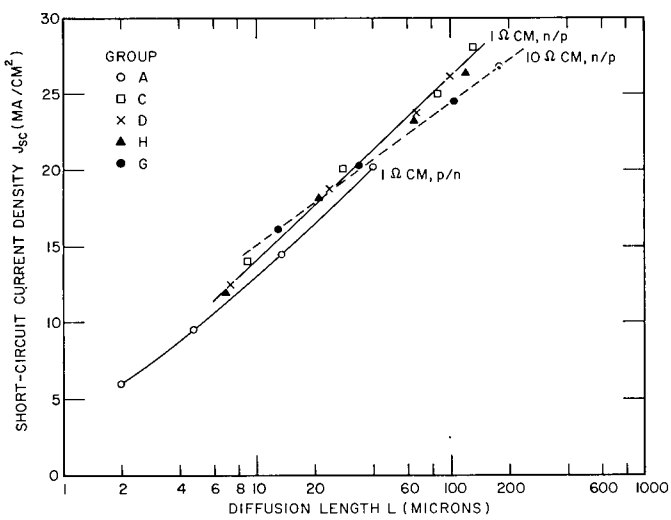

Fig. 60 - Short-circuit current density vs minority-carrier diffusion length of individual solar cells

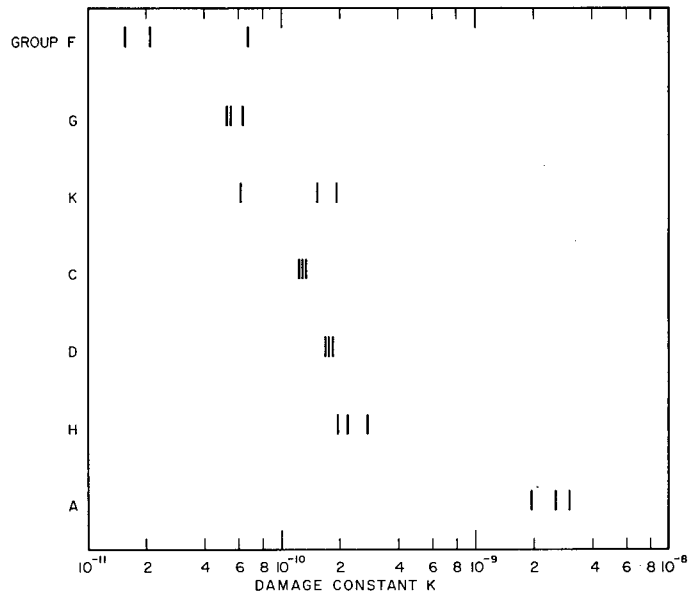

Fig. 61 - Summary of solar-cell damage-constant values

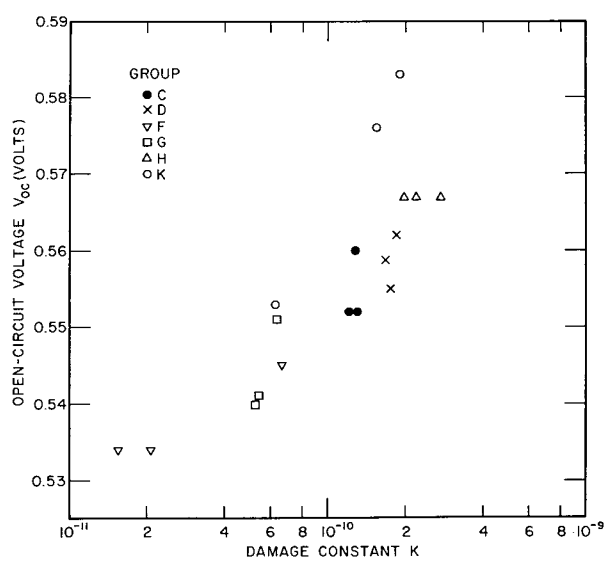

Fig. 62 - Solar-cell open-circuit voltage vs damage constant

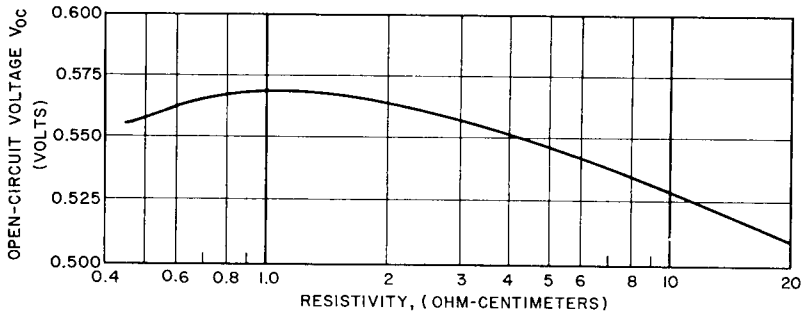

Fig. 63 - Solar-cell open-circuit voltage vs resistivity (12)

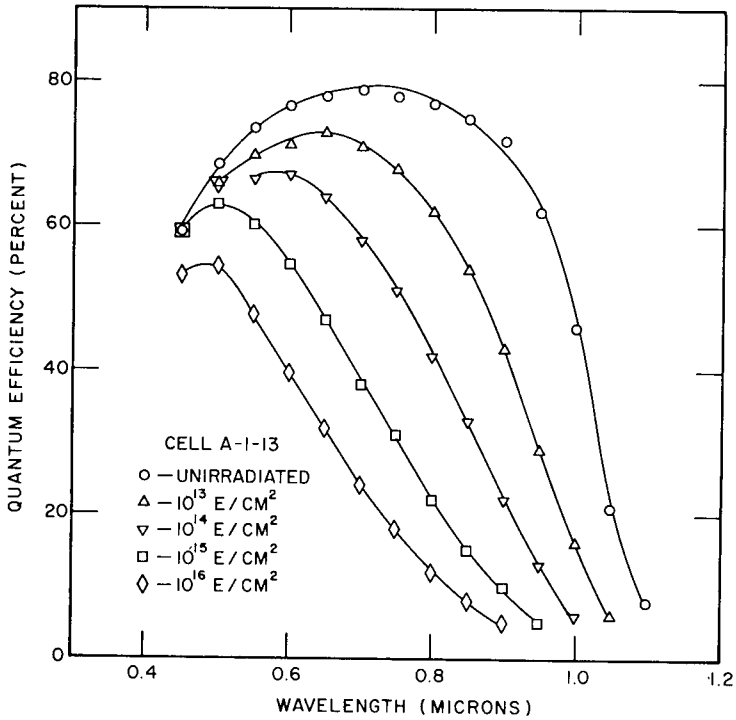

Fig. 64 - Quantum-efficiency degradation of solar cell A-1-13

UNCLASSIFIED

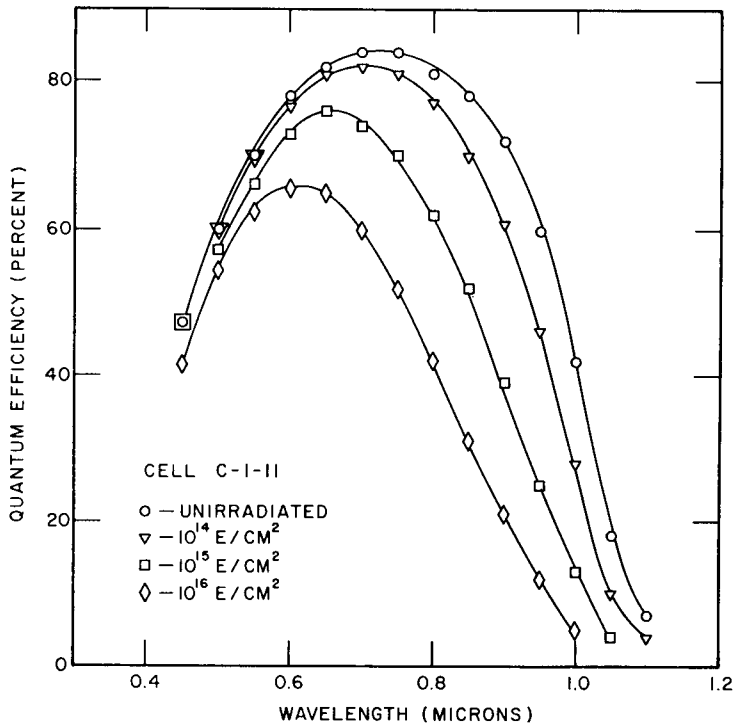

Fig. 65 - Quantum-efficiency degradation of solar cell C-1-11

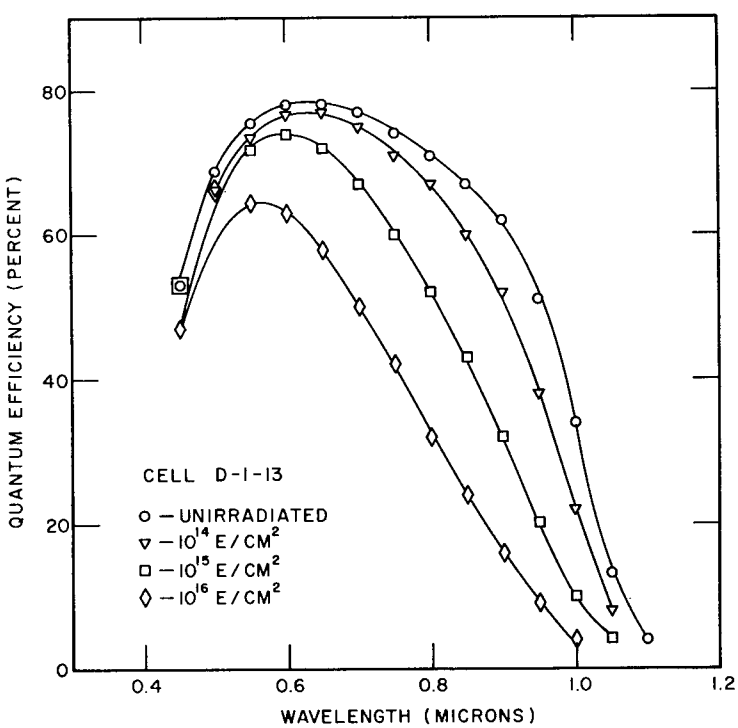

Fig. 66 - Quantum-efficiency degradation of solar cell D-1-13

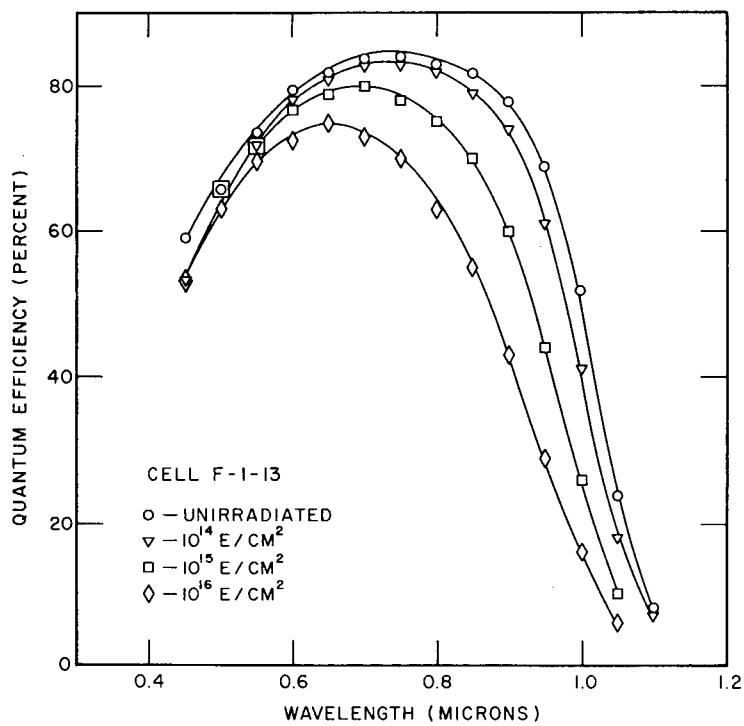

Fig. 67 - Quantum-efficiency degradation of solar cell F-1-13

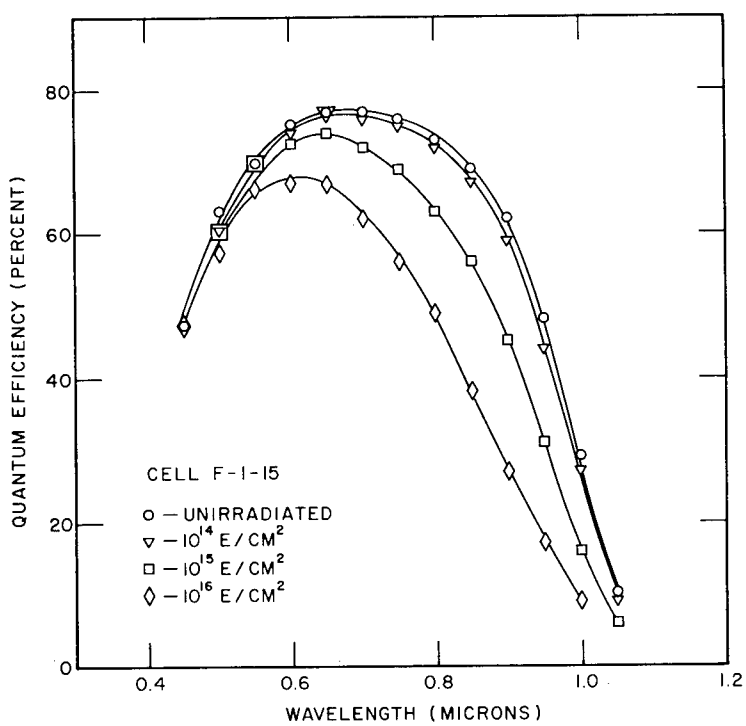

Fig. 68 - Quantum-efficiency degradation of solar cell F-1-15

UNCLASSIFIED

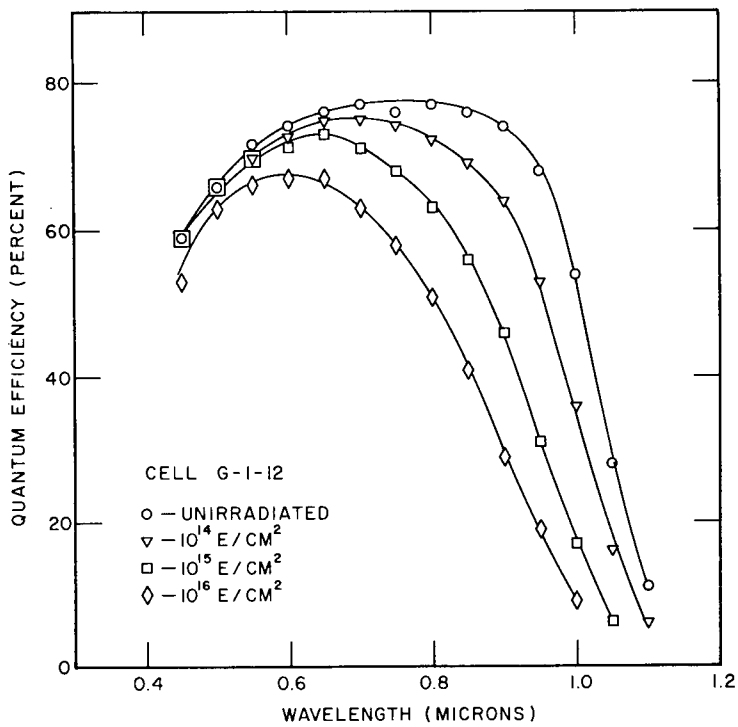

Fig. 69 - Quantum-efficiency degradation of solar cell G-1-12

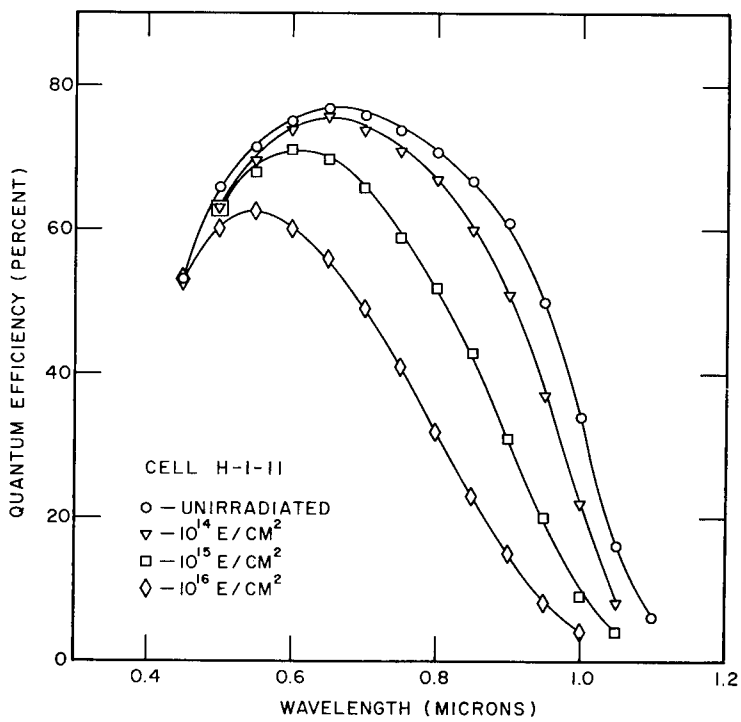

Fig. 70 - Quantum-efficiency degradation of solar cell H-1-11

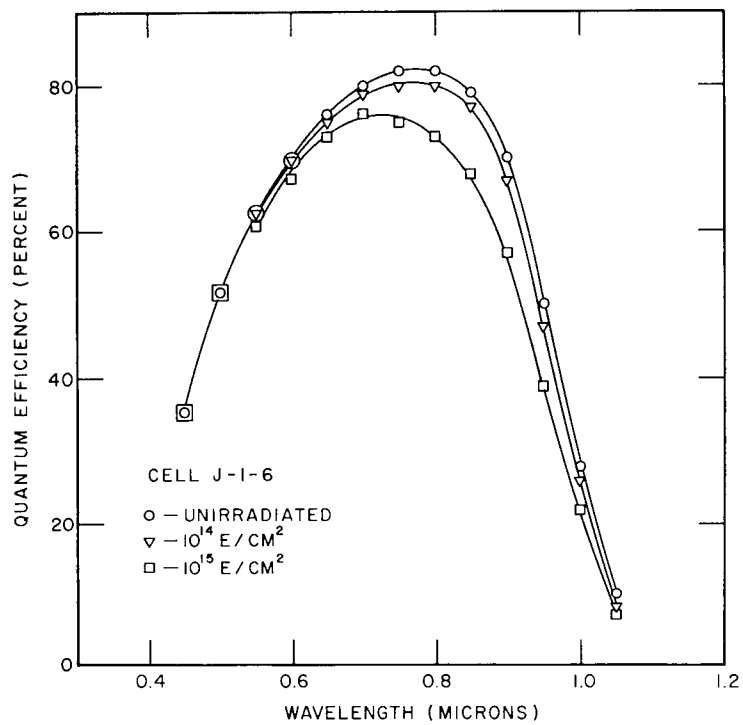

Fig. 71 - Quantum-efficiency degradation of solar cell J-1-6

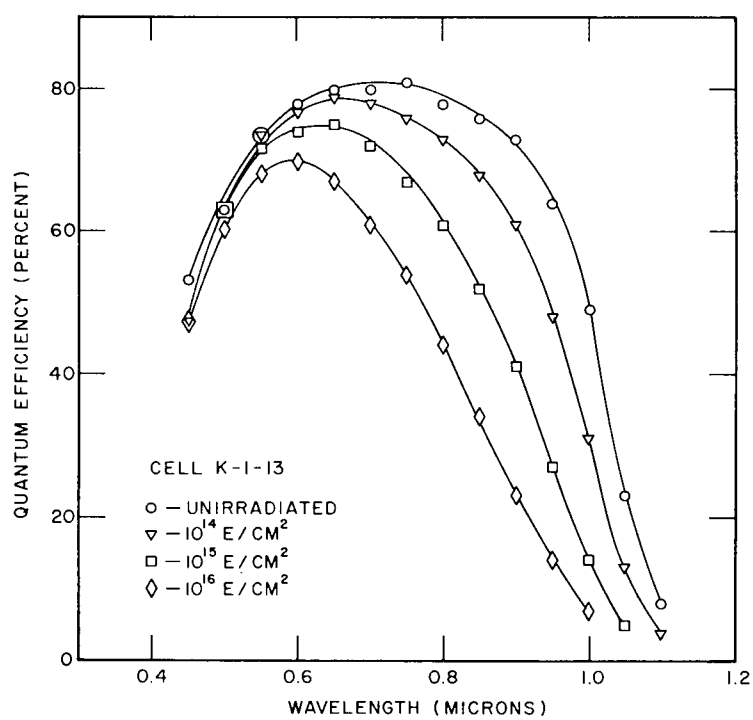

Fig. 72 - Quantum-efficiency degradation of solar cell K-1-13

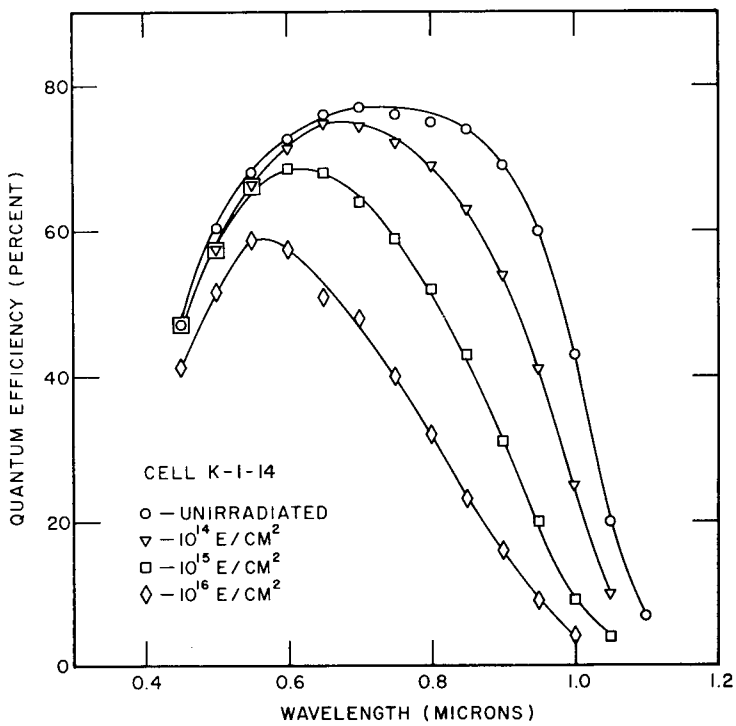

Fig. 73 - Quantum-efficiency degradation of solar cell K-1-14